Periodica Polytechnica
Civil Engineering

x(y) pp. x-x, (year)
DOI: 10.3311/PPci.XXXX


RESEARCH ARTICLE

# Optimal fire design of steel tapered portal frames

Tamás Balogh[1], László Gergely Vigh[1]

Received xx Xxxx 201x

***Abstract***
*The development of new and valuable conceptual design concepts based on structural optimization results is the global aim of the presented research in order to assist the industry in economical fire design of steel tapered portal frames. In order to find optimal configurations regarding the life cycle of the structure, a complex, reliability based structural optimization framework has been developed for tapered portal frame structures. Due to the high nonlinearity and discrete nature of the optimality problem, Genetic Algorithm is invoked to find optimal solutions according to the objective function in with the probability of failure is evaluated using First Order Reliability Method. The applied heuristic algorithm ensures that a number of possible alternatives are analysed during the design process. Based on evaluation of the results of a parametric study, new conceptual design concepts and recommendations are developed and presented for steel tapered portal frames used as storage hall related to optimal structural safety, common design practice and optimal structural fire design.*

***Keywords***
*Structural optimization, Fire design, Steel frames, Reliability based optimization*

[1]Department of Structural Engineering
Faculty of Civil Engineering,
Budapest University of Techology and Economics
H-1111 Budapest, Műegyetem rkp 3., Hungary (e-mail: balogh.tamas@epito.bme.hu, vigh.l.gergely@epito.bme.hu)

## 1 Introduction

Tapered portal frames are commonly applied for single storey industrial buildings all over the globe due to their economical material consumption. It would be favourable to understand clearly from economical point-of-view how cheaper or more reliable frames can be designed and constructed. A number of studies [1-8] exist related to the optimization of regular or tapered portal frames considering only gravitational and meteorological loads in order to achieve a more economic design usually by minimizing the weight or the initial cost of the structure. However, since the introduction of European standards, designers have to satisfy the reliability of structures according to stricter requirements. Among others, extreme effects, such as seismic or fire effects came to the fore.

Papers, dealing with optimal design of tapered frames against extreme effects, can be hardly found in the literature. In case of seismic design, [9] discusses reliability based optimal design of tapered portal frame structures, other available studies mainly investigate multi-story braced or moment resisting frames (e.g. [10, 11, 12]). In case of fire design, [13] presents optimal solutions for a simple single-storey frame constructed using conventional square hollow sections. Particle swarm optimization technique was applied in order to minimize the objective function which expressed the initial cost of the structure. The author derived the optimization constraints according to the formulae of Eurocode standards [14, 15], while the internal forces in the elements were calculated using first order theory and the gas temperature was calculated using ISO standard fire curve [16]. The author concluded that with the use of passive fire protection significant cost savings can be achieved. The amount of achievable saving is strongly dependent on the required fire resistance time. Comparing with the investigation in this paper, the presented research uses performance based design concept, more realistic description of fire event and more complex nonlinear structural analysis methods. In [17], reliability based optimization of tapered portal frame structures is discussed for some cases in order to provide solutions having both low initial cost and acceptable structural performance in fire design situation. Based on the results of a parametric study, the authors could draw valuable observations related to the fire design of such structural solutions. It was shown that the maximum temperature, the shape of fire curve and the duration of the flashover phase have a significant effect on the structural reliability and the optimal solutions. Furthermore, the authors pointed that without passive protection economical configuration cannot be achieved due to the fact that without any protection the steel reaches high temperature within a short time.

As for the structural optimization of reinforced concrete structures, in [18] the authors present lifetime cost optimization of simply supported one-way concrete slabs which are exposed to fire. Contrary to the problem of tapered portal frame structures, the failure of one-way concrete slabs can be easily formulated through analysing the equilibrium of the critical cross section. In [18] a correct mathematical formulation is given to the investigated problem based on an extensive literature review. The probability of structural fire was obtained using ISO standard fire curve. The authors provide graphs in order to help to select economically optimal solutions for different design cases. It was shown that additional investments in structural safety can result cost-effective solutions for the lifetime of the structure especially in the case high failure losses compared to the initial investments.

The lack of available information related to the optimal fire design of steel tapered portal frames motivated this research because there is no study focusing on structural fire optimization of tapered portal frame structures. The connection of structural optimization framework with complex and comprehensive reliability calculation framework for fire effects is new and cannot be found in the published literature. State-of-the-art analysis and assessment tools are incorporated in the optimization algorithm and objective function evaluation. The presented results provide information about the optimal safety level, the safety and reliability of common design practice and the design concepts which can be used directly by structural fire design.

## 2 Investigated structural configuration

In this study, the optimal design of steel tapered portal frame is investigated on the basis of optimization results related to a basic configuration (in Fig. 1) with the help of a numerical algorithm framework. The structure is divided into two fire compartments; the first one is considered to be a small office, while the second part with 36 m total length has storage hall function.

The tapered primary frames are welded; the steel grade is selected for S355J2 structural steel (with 355MPa yield strength). The secondary elements (e.g. wind bracing) are constructed from S235 steel grade using prefabricated, tension-only solid round bar sections. From the point-of-view of structural fire design, the dimensions of the main frames and the appropriate thickness of the fire protection are considered design variables. The presented structure was investigated from different perspectives in the framework of HighPerFrame RDI project [19].

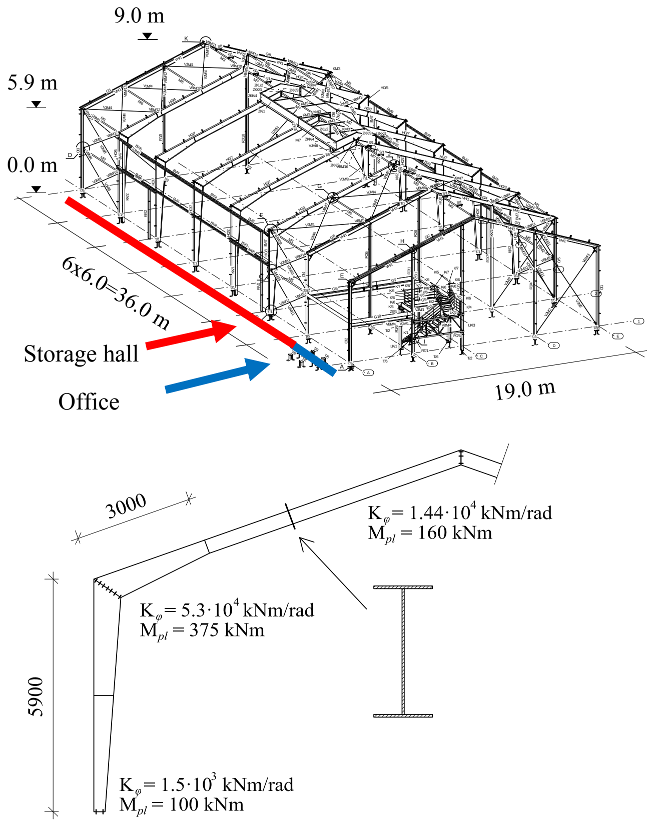


**Fig. 1** Basic configuration of the investigated structure with the connection parameters

Based on the outcomes of a refined numerical study [20], the base connections can be considered as pinned connections while the beam-to-beam and beam-to-column are rigid connections according to the guidelines of MSZ EN 1993-1-8:2012 (EC3-1-8) [21] standard. The actual properties of the connections are taken into consideration within the nonlinear structural analysis, as it is described in [22]. The columns are restrained against Lateral Torsional Buckling (LTB) approximately at the middle of the eave height, while there are altogether six brace element equally distributed in the roof level in order to support the compressed flange of the beam elements. At high temperatures, the sheeting and purlins cannot be considered as supports for the flanges; they lose their stiffness very quickly because of the high section factor and the thin walls.

In this study, intumescent coating fire protection is applied due to the facts that painting is practical, aesthetic and easy to use. The properties of a specific product, namely Polylack A paint [23] of Dunamenti Tűzvédelem Hungary Ltd., are considered in the calculations. However, the calculated paint thicknesses can be converted if a different product is used; the only criterion is that the prescribed thicknesses in the design sheet (where the minimum paint thickness is given as a function of section factor for a given critical temperature, e.g. for 550C°) need to be given according to MSZ EN 13381-8 [24] standard. While an iterative algorithm is given in MSZ EN 1993-1-2:2013 (EC3-1-2) [15] to calculate the steel temperatures for unprotected and protected steel sections, the standardized closed formulae cannot be used because the thermal properties and the exact thickness of the intumescent paint is not known during fire exposure. The everyday practice selects the appropriate thickness from the design sheets only based on the critical temperature and the section modulus. Thus, no closed formula exists to calculate the temperatures of a steel plate. In this study, the iterative algorithm of [15] is adopted in the algorithm and the necessary so-called equivalent constant thermal resistance [25] is calculated based on an ECCS (European Conventions for Constructional Steelwork) recommendation [26, 27] and on data given in the design sheet [23].

## 3 Optimization problem

### 3.1 Description of the optimality problem

In most of the cases in the available literature, the aim of structural optimization studies is to find structural configurations with minimum structural weight or minimum initial cost. These solutions are often considered as the possible cheapest solutions. Considering extreme (seismic effects, fire effects, etc.) and not conventional loading conditions, the cheapest configuration may be the one which gives the minimum cost considering the life cycle of the structure, the risk of different damage states and the amount of total losses, because in case of extreme effects the losses can be far more significant than under conventional loading conditions.

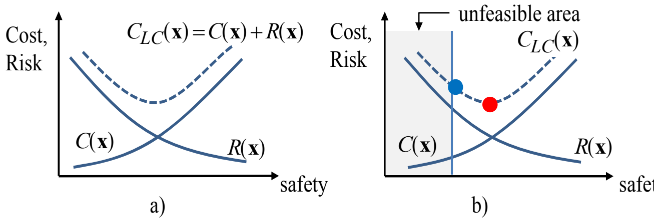


**Fig. 2** Optimal design concept: a) interpretation of life cycle cost; b) life cycle optimum

In some cases the structural reliability may be significantly increased with slight increase of the initial cost. This is illustrated in Fig 2b, where the red point indicates the optimal configuration having the sum of cost ($C(\mathbf{x})$) and risk ($R(\mathbf{x})$) minimum, the blue point shows feasible optimum having minimum initial cost and maximum acceptable risk according to the standard, e.g. MSZ EN 1990:2011 (EC0) [28]. The risk of a failure means the risk of a failure in fire design situation in this case. The dashed line ($C_{LC}(\mathbf{x})$) is the so-called life cycle cost (Fig. 2a). The aim of life cycle cost optimization is finding a solution with minimal life cycle cost:

$$min!\,C_{LC}(\mathbf{x}) = min!\,[C(\mathbf{x}) + R(\mathbf{x})] \qquad (1)$$

where $\mathbf{x}$ is a vector containing the design variables. For this reason, it can be stated that the optimality problem is discrete because available dimensions of steel plates and possible thicknesses of fire protection are discrete; and highly nonlinear due to the fact that the fire design, the structural behaviour in fire and the reliability calculation are highly nonlinear.

### 3.2 Description of the optimality problem

The objective function expresses the life cycle cost of the optimized structure. In [29] the authors presented a possible way for formulation of life cycle cost of the investigated structure based on [30]. $C_{LC}(\mathbf{x})$ can be formulated in the following way:

$$C_{LC}(\mathbf{x}) = \underbrace{C_0(\mathbf{x}) + C_1(\mathbf{x}) + C_2}_{C(\mathbf{x})} + \ldots$$
$$+\underbrace{\begin{matrix} C_f \cdot P_{failure}(\mathbf{x}) + 0.01C_f \cdot P_{ignition} + \ldots \\ + 0.05C_f \cdot P_{ignition+intervention} \end{matrix}}_{R(\mathbf{x})} \qquad (2)$$

In Eq. (2), $C_0(\mathbf{x})$, $C_1(\mathbf{x})$ and $C_2$ are the initial cost of steel superstructure, the cost of passive protection and the cost of active safety measures, respectively, while $C_f$ and $P_{failure}(\mathbf{x})$ refer to total losses and the failure probability related to the service life that is equal to 50 years. The last two terms express the damage cost which is caused by moderate fire (quenched before flashover) and by intervention (e.g. damage caused by sprinkler system and/or fire fighting). $C_f$ contains direct (e.g. value of stored material or the construction of a new storage hall) and indirect cost components (e.g. missing income or malfunction in production). The optimal solution is associated with a structure that results minimum $C_{LC}(\mathbf{x})$. The minima of Eq. (2) objective function need to be found using a method which is able to handle the high nonlinearity and the discrete nature of the problem.

A number of components in Eq. (2) depend on the value of design variables, for example, if the thickness of the flanges or passive fire protection is increased, this increment will directly change the $C_0(\mathbf{x})$ or $C_1(\mathbf{x})$ cost components. Furthermore, in case of a stronger or a better protected frame the failure probability is lower compared to a less protected one and the risk of the structural failure in fire design situation is decreased.

The initial cost is proportional to the weight of the frame:

$$C_0(\mathbf{x}) = n_f \sum_{i=1}^{n_p} b_i \cdot t_i \cdot l_i \cdot \rho \cdot c_s + \dots$$
$$+ \sum_{i=1}^{n_b} \frac{d_i^2 \cdot \pi}{4} \cdot l_i \cdot \rho \cdot c_s + C_{sh} \quad (3)$$
$$b_i, t_i, l_i, d_i, l_i \in \mathbf{x}, \forall i$$

This approach is clearly an approximation; however, it is often used by industrial representatives in cost calculations and bids. In Eq. (3), $n_f$, $n_p$, $c_s$ and $C_{sh}$ are the number of frames, the number of steel plates of a frame, cost rate in €/kg unit and the cost of the sheeting and bracing system. The weight of the $i^{th}$ plate is calculated by multiplying $b_i$ (width), $t_i$ (thickness), $l_i$ (length) and $\rho$ (density). The $n_b$ and $d_i$ are the number of bracing elements and the diameter of $i^{th}$ steel bar, respectively. Due to the fact that column base connections are pinned, the dimensions of foundation are not design variables and the cost of foundation is not considered in this study.

The cost of the passive fire protection is considered to be proportional to the protected surface, thus it can be formulated as follows:

$$C_1(\mathbf{x}) = n_f \sum_{j=1}^{n_e} A_j \cdot l_j \cdot t_{p,j} \cdot c_p \qquad t_{p,j} \in \mathbf{x}, \forall j \quad (4)$$

where $n_e$ is the number of protected elements, $A_j$ is the protected surface of the $j^{th}$ element, $l_j$ is the length of the $j^{th}$ element, $t_{p,j}$ is the protection thickness on the $j^{th}$ element and $c_p$ is the cost rate in €/(mm·m$^2$) unit.

### 3.3 Fire effects

The fire effect and its severity are represented in the method through the so-called fire curve: as temperature curve as a function of the time (Fig. 3). Different fire curves are used in design practice among which some represents only a comparable effect (e.g. ISO standard fire curve [16]) and do not intend to express real and physical effects. Other fire curves which have been obtained with advanced methods and models (e.g. one- and two-zone models [31]) can represent fire severity and temperatures closer to the reality. Realistic modelling of fire effect is an important issue of reliability calculation. The fire effects in this study are modelled with fire curves obtained with the help of OZone V2.2.6 software [31] in order to represent more realistic temperatures than e.g. ISO standard curve. The program is able to consider several influencing parameters, such as the fire load, combustion heat, fire growth rate, ventilation, geometry of the compartment, etc. These parameters may be considered on different values in the parametric study (Section 5).

It is important to note that the temperatures (in Fig. 3) are presented on design value since they are calculated on the basis of parameters from EC3-1-2 considered with their design value. It was assumed that the curve calculated with Ozone represents 95$^{th}$ percentile of the effects [22]. The uncertainties in the steel temperature are considered in the analysis with the help of a global uncertainty factor (Table 1) whose parameters and distribution type was obtained in an earlier study [22]. The temperature input is the mean fire curve (Fig. 8) that is derived from the design curve.

In order to avoid the numerical instabilities within the reliability analysis, the decay period of the curves is neglected and substituted with the maximum gas temperature.

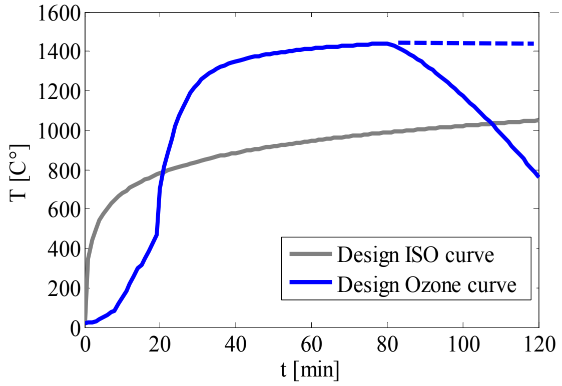


**Fig. 3** The difference between ISO and Ozone fire curves

### 3.4 Reliability analysis and random variables

$P_{failure}(\mathbf{x})$ and $P_{ignition}$ in Eq. (2) are calculated with the help of a complex and comprehensive reliability calculation framework (Fig. 3.) [22]. The specialty of the developed framework is that state of the art analysis methods are incorporated in the reliability analysis and the reliability calculation and the performance evaluation do not focus on a single and separated element but the whole structural system. The limit state function is formulated on time basis because the life and structural safety is verified using time demand (15, 30, 45, etc.) in everyday practice. Fig. 4 proposes a global overview about the reliability calculation. Only the relevant aspects of the method are mentioned and described, for further information refer to [22]. The annual ignition occurrence is calculated with the help of an event tree, similarly to [32]. The $P_{FL|A}$ is the probability of growth of the fire into flashover when active safety measure is applied. According to [32], $P_{FL|A}$ equals to 0.02, 0.0625 and 1.0 in case of fire extinguish system (sprinkler), smoke detection system and no applied safety measure, respectively.

The occurrence of ignitions and the possibility of growth into a fully developed fire are taken into account within a Bayesian network [33]. The failure probability is calculated according to the conditional probability rule:

$$P_{failure}(\mathbf{x}) = P_{failure|flashover}(\mathbf{x}) \cdot P_{flashover} \quad (5)$$

The conditional probability ($P_{failure|flashover}(\mathbf{x})$) is the outcome of a reliability analysis that is based on First Order Reliability

Method (FORM) [33]. Due to the fact that some of the random variables are not normally distributed and possibly correlated, Hasofer-Lind-Rackwitz-Fiessler iteration [34] is adopted in the algorithm. The limit state function gives the D/C ratio (demand-to-capacity ratio) of the frame in time unit, the evaluation methodology incorporates three main steps, i.e.: 1) calculation of element temperatures in every 10, 20, etc. seconds depending on the investigated time range and the size of the time-step; 2) evaluation a structural analysis in OpenSees Thermal [35] considering dead, meteorological, live loads and the steel temperatures in every time-step; 3) evaluation of the load resistance capacity of the structure in every time-step according to MSZ EN 1993-1-1:2009 (EC3-1-1) [36] and EC3-1-2 [15] using the calculated temperatures and internal forces from time-step structural analysis [22]. The considered failure modes are the follows:

- strength and stability failure of beam and column elements;
- shear buckling of the web plates;
- plastic sway mechanism by the plasticity of the connections.

In case of strength and stability verification, the so-called General Method of EC3-1-1 is adopted in the algorithm in which the in-plane stability failures are considered via geometrically nonlinear analysis on imperfect model, while the reduction factor method [36, 15] is used for verification out-of-plane stability failure modes (Fig. 4). The steps of the procedure are presented in Fig. 4 and explained in details in [22].

**Fig. 4** Overview from the proposed methodology and the limit state function

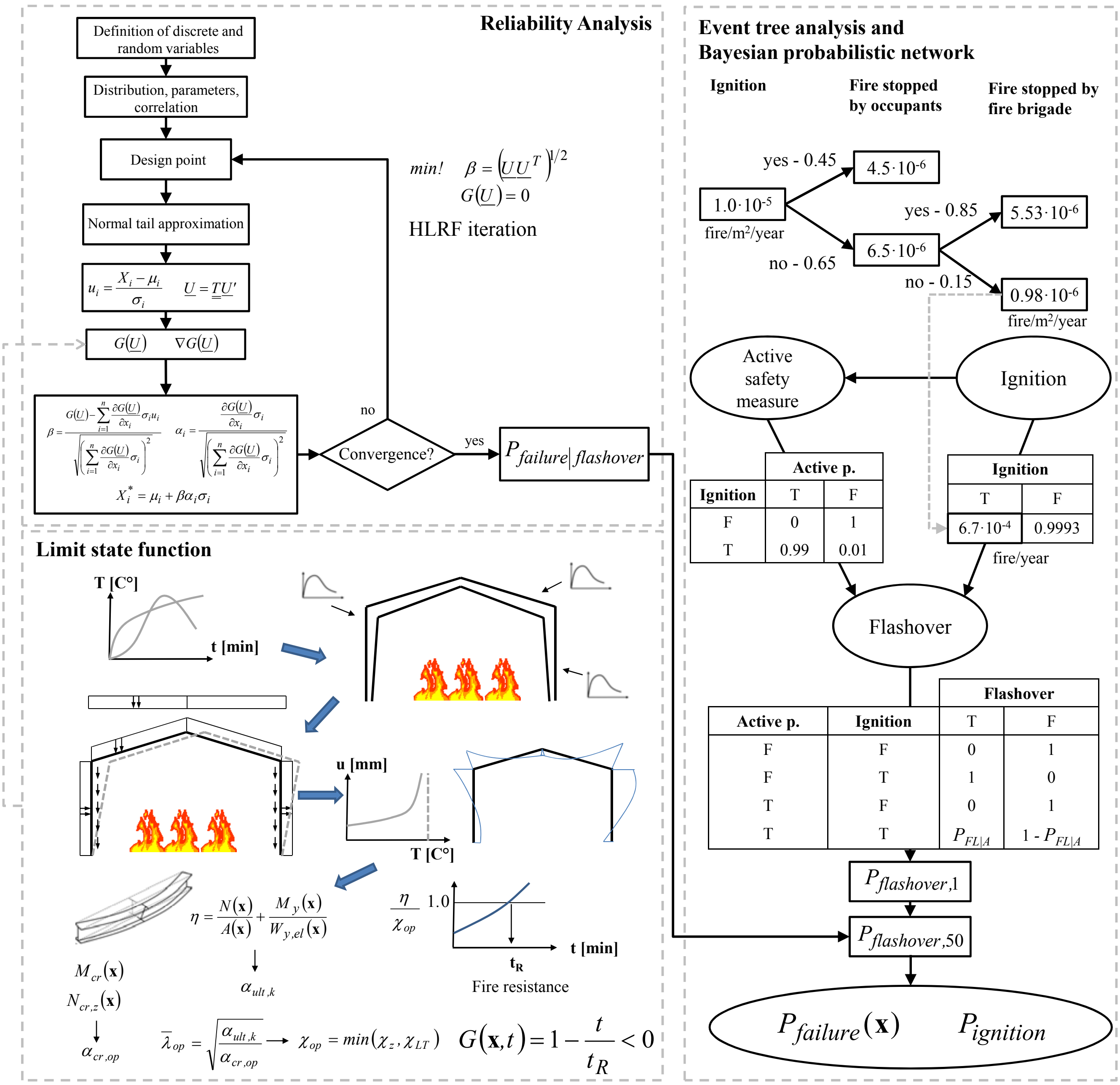

For sake of simplicity the reliability analysis is based on two-dimensional structural analysis of an individual frame, however, the structure (Fig. 1) contains altogether seven frames in the investigated compartment. We consider the whole structure to be failed if the failure of one frame occurs. For this reason a system of frames is a series reliability system, where the failure of frames is correlated. There are formulae which give approximation for the lower and upper limits of the system failure probability, however in case of these limits [33] only no or full correlation can be taken into account. To consider the correlation among the frames, other approximation may be used where the system failure probability and reliability index are calculated with the use of multivariate normal probability distribution function:

$$\beta_{S,failure|flashover} \cong -\boldsymbol{\Phi}^{-1}\left(P_{S,failure|flashover}\right) = \\ = -\boldsymbol{\Phi}^{-1}\left(1-\boldsymbol{\Phi}_m\left(\boldsymbol{\beta},\boldsymbol{\rho}\right)\right) \tag{6}$$

In Eq. (6), the $\boldsymbol{\Phi}$, $\boldsymbol{\Phi}_m$, $\beta_{S,failure|flashover}$ and $P_{S,failure|flashover}$, are the single- and multivariate standard normal cumulative distribution functions, the so-called reliability index ($P = \Phi(-\beta)$) of the system and the probability of failure related to the system. Obviously, the conditional probability shall be substituted and not the probability which contains the ignition. The $\boldsymbol{\beta}$ and $\boldsymbol{\rho}$ are the reliability index vector with the reliability indices of individual frames and correlation matrix in the following form, where the $n$ is the number of frames:

$$\boldsymbol{\beta} = \begin{bmatrix} \beta_{1,failure|flashover} \\ \beta_{2,failure|flashover} \\ \ldots \\ \beta_{n,failure|flashover} \end{bmatrix} \\ \boldsymbol{\rho} = \begin{bmatrix} 1 & \rho_{12} & \ldots & \rho_{1n} \\ \rho_{21} & 1 & \ldots & \rho_{2n} \\ \ldots & \ldots & 1 & \rho_{3n} \\ \rho_{n1} & \rho_{n2} & \rho_{n3} & 1 \end{bmatrix} \quad \rho_{ij} = \rho_{ji} \tag{7}$$

In case of the investigated structure, $n$ is set to 5 since the first and last frames are exposed to less severe effects due to their spatial location. The results of preliminary calculations showed (Fig. 5, where $\rho_{ij}=\rho_{ji}=\rho$ and $\beta_{i,failure|flashover}=1.0$) that the system reliability significantly depends on the correlation coefficient, however, in case of low correlations this dependence is not so significant. Some random variables are supposed to be highly correlated, such as strength, section dimensions of the frames and the intensity of meteorological loads, however, due to the following reasons the correlation among the frames is supposed to be low (namely $\rho$=0–0.6): I) there is a spatial variation in the location of the combustible material; II) all of the frames may not be exposed to fire at the same time; III) it is very likely that the temperature varies spatially; IV) there is a certain spatial variation in the equipment load. In order to cover a wide range of possible outcomes, in this study the system reliability is calculated by use of Eq. (7) considering a low $\rho$=0.4 and a considerably high $\rho$=0.9 correlation among the failure of the frames.

The random variables, considered in the reliability analysis, are shown in Table 1. Due to the small variation and the fact that their effect on the global behaviour is small, the uncertainty in the Young's modulus and global geometry is neglected. Among the loads, the weight of equipment (as permanent load) and the meteorological loads, namely wind and snow loads, were considered as random variables. Because of the accuracy in manufacturing and assembly the uncertainty in dead loads are negligible. The uncertainty of yield strength, section moduli and connection parameters has been selected according to the Probabilistic Model Code of Joint Committee on Structural Safety (JCSS) [37]. The CoV (Coefficient of Variation) values related to the section modulus factor are slightly higher in Table 1 than in JCSS because of the tapered elements. $\rho$=0.7 correlation is considered among the section modulus factors.

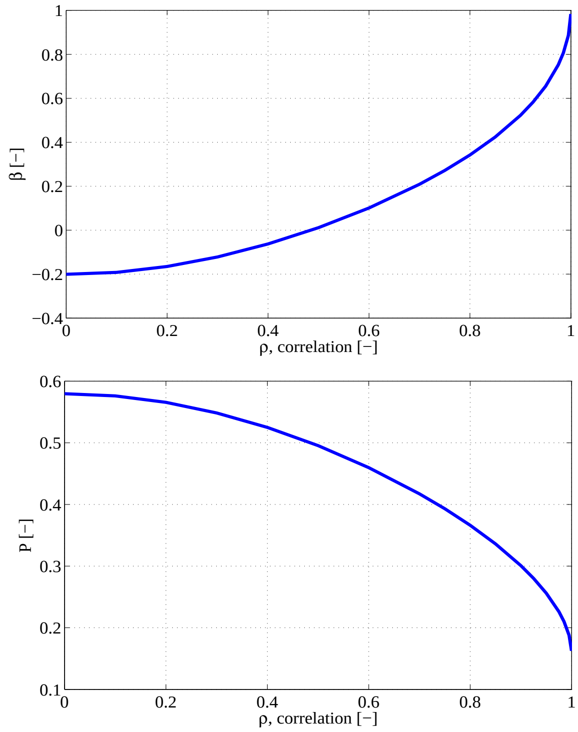


**Fig. 5** The effect of correlation among the components in case of a series reliability system

The reliability problem is time-variant because the meteorological loads vary in time. In order to reduce the complexity of reliability analysis, the problem is transformed into a time-invariant problem with the help of the so-called Turkstra's rule [37], its application is presented for similar problem in [42]. The leading action, i.e. the fire effect, is considered with its lifetime (50 years) maximum, while snow and wind loads are accounted with the distributions of daily maximums. The distributions of daily maximums are derived from meteorological data (wind speeds and snow water equivalents) that have been downloaded from CARPATCLIM database [41] (where different meteorological data sets of Carpathian basin are given for 50 years in 10 km by 10 km grid). The aim was to obtain distributions giving the standardized characteristic load intensities according to the values and instructions of the EN standards (theoretically the provided characteristic load intensities have 0.02 annual exceedance probability), i.e. EC0 [28], MSZ EN 1991-1-3:2005 [38] and MSZ EN 1991-1-4:2007 (EC1-1-4) [39]. The calculation related to the wind loads can be seen in Fig. 6. The characteristic value of variable actions on buildings is defined

**Table 1** Random variabless

| Random Variable | μ | CoV | Distribution | Reference |
|---|---|---|---|---|
| **Yield stress [MPa]** | 388 | 0.07 | Lognormal | [37] |
| **Equipment [kN/m²]** | 0.2/0.5 | 0.2 | Normal | |
| **Wind load [kN/m²]** | 0.06 | 1.963 | Lognormal | Calculation, [37, 28, 39] |
| **Gust coefficient [-]** | 2.463 | 0.15 | Lognormal | [37] |
| **Pressure coefficient [-]** | 1 | 0.2 | Lognormal | [37] |
| **Roughness coefficient [-]** | 0.877 | 0.15 | Lognormal | [37] |
| **Wind velocity [m/s]** | 3.552 | 0.65 | | [41] |
| **Snow load [kN/m²]** | 0.205 | 1.03 | Weibull | Calculation, [28, 38, 40] |
| **Resistance factor for the column-base connection [-]** | 1.25 | 0.15 | Lognormal | [37] |
| **Resistance factor for the column-beam connection [-]** | 1.25 | 0.15 | Lognormal | [37] |
| **Resistance factor of ridge beam-beam connection [-]** | 1.25 | 0.15 | Lognormal | [37] |
| **Right column section modulus factor [-]** | 1 | 0.05 | Normal | [37] |
| **Left beam section modulus factor [-]** | 1 | 0.05 | Normal | [37] |
| **Right beam section modulus factor [-]** | 1 | 0.05 | Normal | [37] |
| **Effect model uncertainty factor [-]** | 1 | 0.15 | Lognormal | |
| **Resistance model uncertainty factor [-]** | 1 | 0.2 | Lognormal | |
| **Model uncertainty in LTB reduction factor -** $\chi_{LT}$ | 1.15 | 0.1 | Normal | [50] |
| **Model uncertainty in FB reduction factor -** $\chi_z$ | 1.15 | 0.1 | Normal | [50] |
| **Steel temperature uncertainty factor [-]** | 1 | 0.3 | Lognormal | [22] |

as a value which has 0.02 exceedance probability within 1 year reference period [28]. In case of the wind load, firstly, the yearly maximum wind velocities were selected in each grid (the data set contained data from 50 years). Using annual maximums, extreme distribution (as the limiting distribution for the maximum or the minimum of a large set of random observations) was fitted on the data in order to find the wind speed which has exactly 0.02 annual exceedance probability. The basic wind velocity in Hungary is $v_{b0}$=23.6 m/s, so the node was selected which results the same velocity as characteristic value (Fig. 6a). Daily maximum wind velocities of 50 years related to the selected node (Fig. 6b) were used in calculation of the distribution. Lognormal distribution (Fig. 6c) was selected to describe the variability in the daily maximum wind velocities.

According to the recommendations of JCSS [37], uncertainties were considered (Table 1) in gust ($c_g$), pressure ($c_p$) and roughness coefficients ($c_r$). The wind pressure of [39] can be formulated as follows using the above mentioned coefficients:

$$q_p(z) = (1 + 7I_v(z)) \cdot \frac{1}{2} \cdot \rho \cdot v_m^2(z) = c_g \cdot \frac{1}{2} \cdot \rho \cdot v_m^2 \qquad (8)$$

In Eq. (8), $I_v$, $\rho$ and $v_m$ are the turbulence intensity, the air density (1.25 kg/m³) and mean wind velocity, respectively. The height (z) is known, namely it is equal to the eave height of the frame (Fig. 1). The pressure coefficient ($c_p$), which is also uncertain (Table 1), takes into consideration the uncertainty of the pressure calculation, so Eq. (8) should be multiplied with it. The mean wind velocity can be calculated as follows [37]:

$$\begin{aligned} v_m(z) &= c_r(z) \cdot c_0(z) \cdot v_b = \\ &= c_r \cdot c_0 \cdot c_{dir} \cdot c_{season} \cdot v_{b0} \end{aligned} \qquad (9)$$

where $c_0$, $c_{dir}$, $c_{season}$ and $v_{b0}$ are orography, directional, season factors and the basic wind velocity, respectively. Further details can be found in EC1-1-4 standard.

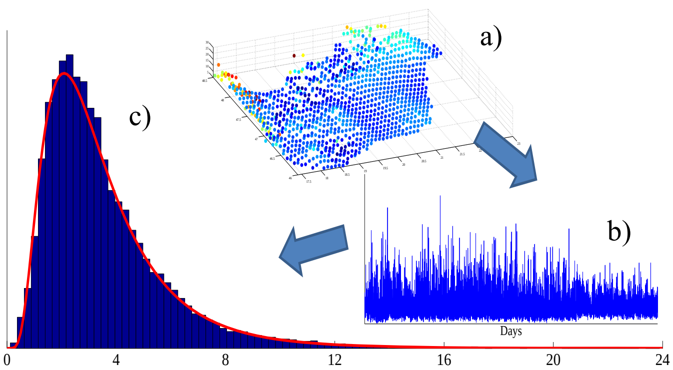


**Fig. 6** Evaluation of the distribution of daily maximum wind speeds: a) EN conforming characteristic wind speeds in Hungary; b) daily maximum wind speeds for 50 years at the selected coordinate; c) fitted distribution

In case of the snow loads, similar procedure is carried out in order to obtain the distribution of daily values that fits to the standardized characteristic load [38]. It has to be noted that the daily maximums are not independent, however, the application of yearly maximum's distribution is clearly too conservative.

The representation of meteorological loads as stochastic processes would be the most accurate solution, but it would overcomplicate the reliability analysis. Calculations showed that application of daily maximums serves internal forces in better agreement with internal forces calculated using the load combination of EC0 standard for extreme design situations. For this reason, this method leads EC0 conforming design.

The problem should be further divided into two fundamental cases, since in Hungary there is no snow in a significant part of the year. Two independent reliability analyses have to be carried with and without considering snow load in the analysis. The calculated reliabilities can be summed easily if we assume that the ignition and the meteorological loads are independent:

$$P_{failure}(\mathbf{x}) = P_w \cdot P_{failure|flashover|w}(\mathbf{x}) \cdot P_{flashover} + \ldots \\ + P_{w+s} \cdot P_{failure|flashover|w+s}(\mathbf{x}) \cdot P_{flashover} \quad (10)$$

In Eq. (10), $P_w$ is the probability that only wind load acts on the frame and there is no snow load, while $P_{w+s}$ is the probability that wind and snow loads act on the frame at the same time. $P_w$ and $P_{w+s}$ can be derived from the meteorological data sets.

The given description of derivation and consideration of meteorological loads and their distribution within the reliability analysis is applied in order to consider representative meteorological loads which are consistent with standardized reliability level. No correlation is considered between the snow and wind loads since the data are related to different coordinates and snow water equivalents in [41] were predicted by complex models and not measured.

## 4 Optimization algorithm

Throughout the optimization process, we seek the global optimum (minimum in our case) of the objective function which expresses the life-cycle cost (Fig. 2) of the investigated structure. The infeasible solutions are eliminated in the process with the help of equality and inequality constraints. In case of a structural optimization problem, equality constraints may express the equilibrium conditions, so stable solutions are only accepted. Inequality constraints express other design constraints, such as strength and stability checks of the main frame elements in persistent design situation. Solutions which violate the design constraints are also unfeasible and are shown with grey colour in Fig. 2.

The optimality problem is defined as the optimal design of a steel tapered moment resisting portal frame structure. The problem is highly nonlinear, discrete and high number of local optima may exist. The optimization variables are the dimensions of the main frame elements and the thicknesses of intumescent coating (Table 2).

The heuristic Genetic Algorithm (GA) [43] optimization algorithm is invoked to find the optimum because genetic algorithm is able to handle highly nonlinear problems, different optimal solutions in parallel and discrete objective functions, it can scan a very large search space during its operation and its operation can be stable with proper setting. Its applicability to similar [7, 8] and other similarly complex and nonlinear structural problems [44] is confirmed by examples from the published literature.

**Table 2** Optimization variables

| **Column** | |
|---|---|
| $t_{w,c}$ | column web thickness |
| $t_{f,c}$ | column flange thickness |
| $b_c$ | column width |
| $h_{c1}$ | column height at the base |
| $h_{c2}$ | column height at eave |
| $t_{p,c1}$ | intumescent coating thickness on the lower part |
| $t_{p,c2}$ | intumescent coating thickness on the upper part |
| $t_{p,c}$ | intumescent coating thickness in the connection zone |
| **Beam** | |
| $t_{w,b}$ | beam web thickness |
| $t_{f,b}$ | beam flange thickness |
| $b_b$ | beam width |
| $h_{b1}$ | the height of non-tapered beam |
| $h_{b2}$ | beam height at the end of the tapered part |
| $t_{p,b1}$ | on the non-tapered part of the beam |
| $t_{p,b2}$ | on the tapered part of the beam |

During its operation, GA seeks the optimum on heuristic way with the help of modifying, crossing and reconstitution of the initial set of possible solutions in every iteration steps, which are called generations. GA literally imitates the evolution; the best individuals survive and transmit their genes for the newer generations; for this reason the technical terms often have biological origin. The design variables are stored in chromosome-like data structures, i.e. in a series of vectors as follows considering the symmetry of the frame ($n$ is the number of individuals – commonly referred as the population size):

$$\mathbf{X} = \begin{bmatrix} \mathbf{x}_1 \\ \mathbf{x}_2 \\ \ldots \\ \mathbf{x}_n \end{bmatrix} \quad (11)$$

$$\mathbf{x} = \begin{bmatrix} h_{c1} & h_{c2} & b_c & t_{w,c} & t_{f,c} & h_{b1} & h_{b2}\ldots & \\ \ldots b_b & t_{w,b} & t_{f,b} & t_{p,c1} & t_{p,c2} & t_{p,b1} & t_{p,b2} & t_{p,c} \end{bmatrix} \quad (12)$$

The find of global optimum cannot be guaranteed and proved due to the fact that the problem is discrete. However, with good settings of GA can find solutions situated very close to the global optimum, with no difference compared to the global optimum from practical point-of-view. It also has to be noted that the algorithm can handle the constraints only with the help of so-called penalty functions [45]. Using penalty functions the problem can be transformed into unconstrained format:

$$\min! C_{LC}(\mathbf{x}) \cdot g_{SLS}(\mathbf{x}) \cdot g_{ULS}(\mathbf{x});$$
$$g_i(\mathbf{x}) = \begin{cases} 1 & \eta_i(\mathbf{x}) \le \eta_{\lim,i} \\ \eta_i(\mathbf{x})^2 & \eta_{\lim,i} < \eta_i(\mathbf{x}) \end{cases} \tag{13}$$

where $g_{ULS}(\mathbf{x})$ and $g_{SLS}(\mathbf{x})$ are the penalty functions related to ultimate and serviceability limit states related conventional design situation [28]. The $\eta_i$ and $\eta_{lim,i}$ are the calculated and acceptable D/C ratio (1.0, i.e. 100%) in the investigated limit states. Eq. (13) is evaluated in case of every individual and in every generation the individuals are sorted considering this value, as a measure of goodness. In persistent design situation, the following limit states are checked: strength and stability failure of beam and column elements, shear buckling of the web plates, strength failure of joints. In case of the serviceability limit states, only the deflection at the middle cross section of the beam is checked in quasi-permanent design situation [28].

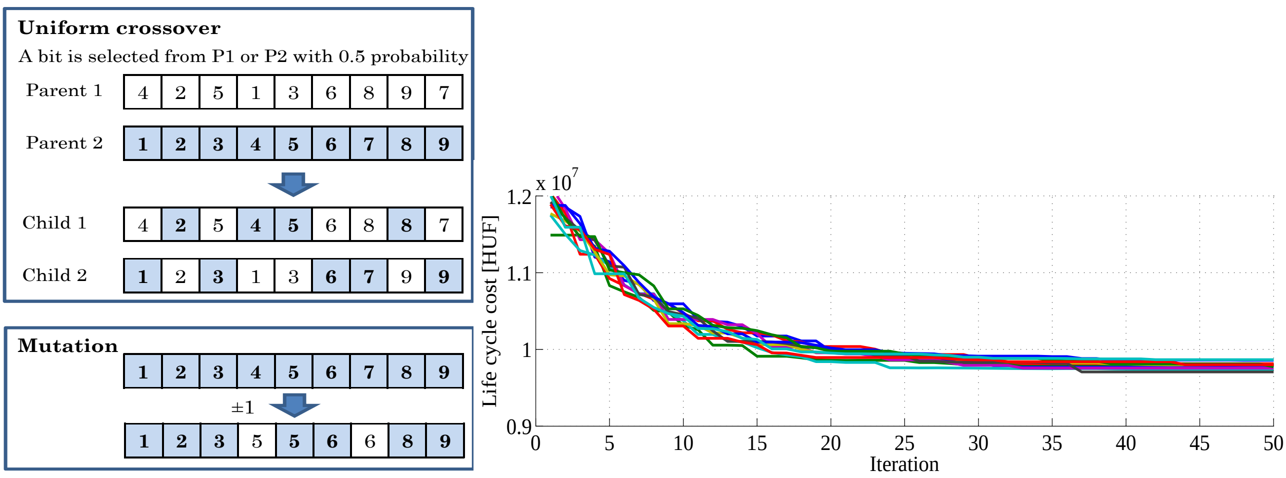


a) b)

**Fig. 7** a) Uniform crossover and mutation operators; b) Convergence of the developed algorithm in case of an example structure

GA starts seeking optimum from a randomly generated initial set; uniform crossover (Fig. 7a) is invoked in the optimization algorithm where the genes of parental individuals are selected randomly with even chance. Crossover ratio controls the percentage of best individuals participating in the crossover. After the crossover the chromosomes are varied further within the mutation procedure. The elite individuals are responsible to preserve the best genomes, thus they are not allowed to be mutated. Mutation (Fig. 7a) ratio gives the number of mutated individuals which are selected randomly excluding the elites, thus one individual may be mutated more than once. The number of mutated genes controls the number of randomly selected and mutated bits. The mutation helps to avoid the local optimum in the optimization process.

In order to find the best settings with reasonable resource needs sensitivity analysis has been carried out. The convergence of the best set is shown in Fig. 7b and in Table 3, respectively, where the results of altogether 11 optimization processes are presented. The algorithm serves consistent results from engineering point-of-view, little scatter appears in the results due to the fact that the problem is extremely nonlinear and the applied population size need to be limited (with the last settings within an optimization process altogether 4900 structures are investigated, which increases the computation time to 70-80 hours). In case of $h_{c2}$, $h_{b1}$, $h_{b2}$, $b_c$, and $b_b$ the observed standard deviation is 2.8-6.7%, which is acceptable from practical reasons and does not mean any difference from designer point of view between the solutions. Due to the fact, that the column base connection is almost pinned, in case of $h_{c1}$ 12.5% standard deviation was obtained because this parameter does not have significant influence on the internal forces and stiffness.

As a final setting, the mutation ratio, number of mutated genes and elite ratio were set to 0.4, 2 and 0.2, respectively. In order to reduce the computational time, the population size is changed dynamically where this parameter set to 200, 40, 20 and 10 in 0-20, 21-30, 31-40 and 41-50 iteration steps, respectively. When the population size is reduced, the best 40, 20 or 10 candidates are kept for further analysis.

**Table 3** Results of sensitivity analysis

| [mm] | $h_{c1}$ | $h_{c2}$ | $h_{b1}$ | $h_{b2}$ | $b_c$ | $b_b$ | $t_{f,c}$ | $t_{f,b}$ | $t_{w,c}$ | $t_{w,b}$ | $t_{p,c1}$ | $t_{p,c2}$ | $t_{p,b2}$ | $t_{p,b1}$ | $t_{p,c}$ |
|---|---|---|---|---|---|---|---|---|---|---|---|---|---|---|---|
| MEAN=9791933 STD=0.485% | 235 | 665 | 230 | 680 | 195 | 180 | 10 | 9 | 6 | 6 | 0.4 | 0.4 | 0.6 | 0.3 | 0.2 |
| | 195 | 670 | 230 | 670 | 195 | 185 | 10 | 9 | 6 | 6 | 0.4 | 0.4 | 0.6 | 0.3 | 0 |
| | 235 | 640 | 230 | 700 | 200 | 190 | 10 | 8 | 6 | 6 | 0.4 | 0.4 | 0.6 | 0.4 | 0 |
| | 240 | 700 | 250 | 725 | 185 | 170 | 11 | 9 | 6 | 6 | 0.4 | 0.5 | 0.6 | 0.3 | 0 |
| | 300 | 595 | 245 | 715 | 200 | 175 | 11 | 9 | 6 | 6 | 0.4 | 0.5 | 0.6 | 0.4 | 0 |
| | 245 | 620 | 225 | 640 | 195 | 175 | 11 | 10 | 6 | 6 | 0.5 | 0.5 | 0.6 | 0.3 | 0 |
| | 195 | 625 | 225 | 665 | 190 | 180 | 11 | 9 | 6 | 6 | 0.4 | 0.5 | 0.6 | 0.4 | 0 |
| | 215 | 590 | 225 | 705 | 190 | 175 | 12 | 9 | 6 | 6 | 0.4 | 0.5 | 0.6 | 0.4 | 0 |
| | 220 | 605 | 240 | 675 | 205 | 180 | 10 | 9 | 6 | 6 | 0.5 | 0.5 | 0.7 | 0.4 | 0.1 |
| | 255 | 665 | 215 | 740 | 195 | 170 | 10 | 9 | 6 | 6 | 0.5 | 0.5 | 0.7 | 0.4 | 0 |
| | 245 | 725 | 200 | 695 | 195 | 165 | 9 | 10 | 6 | 6 | 0.5 | 0.6 | 0.6 | 0.4 | 0.1 |

## 5 Parametric study

The aim of this research is to define new and valuable concepts for fire design of tapered portal frame structures based on the results of structural optimization procedure. In order to give comprehensive and useful concepts, it is important to characterize the sensitivity of the design problem and the optimum on different design parameters, conditions and cost components. For this reason, the achievable optimal solutions are derived in several cases, within the framework of a parametric study.

Table 4 summarizes the investigated cases within the framework of the parametric study. Altogether, the optimal solutions have been obtained in 36 different cases covering a wide range of possible design cases. The listed costs have been obtained with the consideration of Hungarian circumstances based on consultations with practicing engineers. The time demand, the value of cost components, the application of active fire protection, the severity of fire effect and equipment load were varied in this study. Some other parameters like the meteorological loads, the type and the weight of the sheeting system and the main geometry remained to be unchanged.

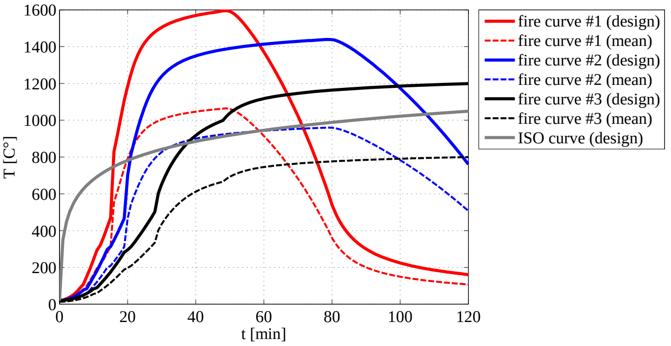


**Fig. 8** Ozone fire curves on design and on mean value

**Table 4** Investigated cases within the parametric study

| | # | Demand (resistance) | $c_s$ [€/kg] see Eq. (3) | $c_p$ [€/ (mm·m²)] see Eq. (4) | $C_2$ [€/m²] see Eq. (2) | Active safety measure | $C_f$ [m €] see Eq. (2) | Fire curve | Equipment [kN/m²] |
|---|---|---|---|---|---|---|---|---|---|
| **A – reference case group** | 1 | R30 | 2.25 | 24 | 40 | smoke detection | 3.0 | 1 | 0.2 |
| | 2 | R45 | 2.25 | 24 | 40 | smoke detection | 3.0 | 1 | 0.2 |
| | 3 | R60 | 2.25 | 24 | 40 | smoke detection | 3.0 | 1 | 0.2 |
| | 4 | R30 | 2.25 | 24 | 40 | smoke detection | 3.0 | 2 | 0.2 |
| | 5 | R45 | 2.25 | 24 | 40 | smoke detection | 3.0 | 2 | 0.2 |
| | 6 | R60 | 2.25 | 24 | 40 | smoke detection | 3.0 | 2 | 0.2 |
| | 7 | R30 | 2.25 | 24 | 40 | smoke detection | 3.0 | 3 | 0.2 |
| | 8 | R45 | 2.25 | 24 | 40 | smoke detection | 3.0 | 3 | 0.2 |
| | 9 | R60 | 2.25 | 24 | 40 | smoke detection | 3.0 | 3 | 0.2 |
| **B** | 10 | R30 | 2.25 | 24 | 40 | smoke detection | 3.0 | 1 | 0.5 |
| | 11 | R45 | 2.25 | 24 | 40 | smoke detection | 3.0 | 1 | 0.5 |
| | 12 | R60 | 2.25 | 24 | 40 | smoke detection | 3.0 | 1 | 0.5 |
| | 13 | R30 | 2.25 | 24 | 40 | smoke detection | 3.0 | 2 | 0.5 |
| | 14 | R45 | 2.25 | 24 | 40 | smoke detection | 3.0 | 2 | 0.5 |
| | 15 | R60 | 2.25 | 24 | 40 | smoke detection | 3.0 | 2 | 0.5 |
| | 16 | R30 | 2.25 | 24 | 40 | smoke detection | 3.0 | 3 | 0.5 |
| | 17 | R45 | 2.25 | 24 | 40 | smoke detection | 3.0 | 3 | 0.5 |
| | 18 | R60 | 2.25 | 24 | 40 | smoke detection | 3.0 | 3 | 0.5 |
| **C** | 19 | R30 | 2.25 | - | 40 | smoke detection | 3.0 | 1 | 0.2 |
| | 20 | R30 | 2.25 | - | 40 | smoke detection | 3.0 | 2 | 0.2 |
| | 21 | R30 | 2.25 | - | 40 | smoke detection | 3.0 | 3 | 0.2 |
| **D** | 22 | R45 | 2.25 | 24 | 40 | smoke detection | 30.0 | 1 | 0.2 |
| | 23 | R45 | 2.25 | 24 | 40 | smoke detection | 30.0 | 2 | 0.2 |
| | 24 | R45 | 2.25 | 24 | 40 | smoke detection | 30.0 | 3 | 0.2 |
| **E** | 25 | R45 | 2.25 | 24 | 40 | smoke detection | 0.3 | 1 | 0.2 |
| | 26 | R45 | 2.25 | 24 | 40 | smoke detection | 0.3 | 2 | 0.2 |
| | 27 | R45 | 2.25 | 24 | 40 | smoke detection | 0.3 | 3 | 0.2 |
| **F†** | 28 | R45 | 4.50 | 48 | 80 | smoke detection | 3.0 | 1 | 0.2 |
| | 29 | R45 | 4.50 | 48 | 80 | smoke detection | 3.0 | 2 | 0.2 |
| | 30 | R45 | 4.50 | 48 | 80 | smoke detection | 3.0 | 3 | 0.2 |
| **G** | 31 | R45 | 2.25 | 24 | - | - | 3.0 | 1 | 0.2 |
| | 32 | R45 | 2.25 | 24 | - | - | 3.0 | 2 | 0.2 |
| | 33 | R45 | 2.25 | 24 | - | - | 3.0 | 3 | 0.2 |
| **H** | 34 | R45 | 2.25 | 24 | 75 | sprinkler system | 3.0 | 1 | 0.2 |
| | 35 | R45 | 2.25 | 24 | 75 | sprinkler system | 3.0 | 2 | 0.2 |
| | 36 | R45 | 2.25 | 24 | 75 | sprinkler system | 3.0 | 3 | 0.2 |

R30, R45 and R60 refer to 30, 45 and 60 minutes time demand, respectively; m EUR refers to million euros.
†A fix cost component, namely the cost of sheeting and bracings, $C_{sh}$, is generally set to 25 €/m², however, in case of group F $C_{sh}$ is set to 50 €/m²

From the point-of-view of the severity of fire effect, altogether three different cases are considered. The fire effect is represented by fire curves (Fig. 8) which have been obtained with the help of two-zone fire model in Ozone V 2.2.6. software [31]. In Fig. 8 the design and mean fire curves are presented and the ISO standard fire curve is also shown as a reference.

The considered three fire design cases are the followings (Fig. 8): 1) extreme (the combustible material is rubber tyre with $q_{f,d}$≈470 MJ/m$^2$ design fire load, with 30 MJ/kg combustion heat [14] and $t_\alpha$=150s fast fire growth rate [14]); 2) severe (the combustible material is rubber tyre and wood with $q_{f,d}$≈670 MJ/m$^2$ design fire load, with ~24 MJ/kg combustion heat on average [14] and $t_\alpha$=200 fast fire growth rate); 3) moderate (the combustible material is wood with $q_{f,d}$≈1070 MJ/m$^2$ design fire load, with 17.5 MJ/kg combustion heat [14] and $t_\alpha$=300 fast fire growth rate[14]).

Within the framework of the presented parametric study the optimal solutions are investigated: I) in case of different demand levels (A case group – reference cases); II) in case of different constructional costs and losses (see D, E and F case groups); III) with different active safety measures (see G and H case groups in Table 4); IV) without passive fire protection (see C case group); V) with different gravity load intensities (see B case group). As the most common fire protection in Hungary, smoke detection device is assumed in most cases as active safety measure. However, the optimal solutions with only passive protection are also analysed.

In order to characterize the importance of proper fire design, the initial cost of optimal solutions for the above listed 36 cases are also obtained without considering fire design situation during the design. The life cycle cost and fire risk related to these solutions are obtained thereafter with passive fire protection selected for $T_{cr}$=500-550 °C critical temperature according to the common fire protection design practice.

## 6 Optimization results

The optimization results are summarized in Table 5. In the first and second columns, the dimensions of cross sections can be seen for both column and beam elements, while in the following columns the thicknesses of intumescent coating fire protection have been presented. The *D/C* column shows the D/C ratio in Ultimate Limit State (ULS), persistent design situation according to the critical failure mode. $\beta_{opt}$ is the reliability index (Section 3.4) related to the optimum safety level which results minimum life cycle cost value ($C_{LC}$). $C_0$ contains the cost of the purlins, the sheeting system and the cost of the bracing system, as well. In order to take into account the whole frame's cost in the calculation the outer frames have been considered with the following dimensions: column: 300-300x6+200x8, beam: 300-300x6+200x8.

The calculated reliability indices, initial and life cycle cost components of cases #1 - #9 show that fire curve #1 is the most demanding from the considered cases, while fire curve #3 represents much less severe fire. Not surprisingly, in case of 45 and 60 minutes time demand levels, the optimized solutions requires more investments regarding to the initial cost of the steel structure and the initial cost of passive protection. Furthermore for R45 and R60, passive protection with thick layers has to be used for good performance and safety. However in case of fire curve #3, when the design aim is to satisfy R30 criterion, there is no need for passive fire protection (see the results of case #7 and #16). Nevertheless, this is not the case for fire curves #1 and #2. By case #19 and #20, because the fire effect is too demanding and the algorithm cannot find good and stable solution. For this reason, it is not safe and economical to ensure the fire safety without passive fire protection (seel also [17]), because the steel plates are very heat conductive and they loss their stiffness and strength very quickly in severe fire.

Generally, the D/C ratio of the frames in persistent design situation is high (Table 5, cases #1 - #36), thus the presented solutions are possible design alternatives. It shows that optimal design against conventional effects and optimal design against extreme effects can be contradictory objectives and the consideration of fire design situation during the seeking optimum solutions during the design process (and not after it) will change the resulted configuration.

The optimized solutions are compared with solutions designed by practicing engineers with C0≈57,000€ (column: 300-700x6+180x10, beam: 380-700x6+165x8) considering 0.2 kN/m2 equipment load, and optimized by the developed algorithm with C0≈55,700€ (column: 185-665x6+205x9, beam: 215-700x6+185x8) and with C0≈56,260€ (column: 130-855x6+210x8, beam: 230-815x6+190x8) considering only serviceability and ULS constraints in persistent design situation for 0.2 kN/m2 and 0.5 kN/m2 equipment load, respectively. The solutions provided in Table 5 have larger $C_0$ cost in most of the cases, however, they have lower $C_1$ cost and they have lower $C_{LC}$ cost in fire design situation (Table 8).

It can be seen from the results that the flanges and webs are less slender (Fig. 9) compared to the width-to-thickness ratio of plates of the optimized reference frames. Probably, the most economical solution cannot be achieved only with protection elements with more slender sections (with higher plate width-to-thickness ratio), which may be optimal and adequate in persistent design situation, using thick passive protection.

| # | $h_{c1}$ - $h_{c2}$ x $t_{w,c}$* + $b_c$ x $t_{f,c}$ | $h_{b1}$ - $h_{b2}$ x $t_{w,b}$* + $b_b$ x $t_{f,b}$ | $t_{p,c1}$ | $t_{p,c2}$ | $t_{p,b2}$ | $t_{p,b1}$ | $t_{p,c}$ | D/C [%] | $\beta_{opt}$ 0.4 | $\beta$ 0.9 | $C_0$ | $C_1$ | $C_2$ | $C_{LC}$ |
|---|---|---|---|---|---|---|---|---|---|---|---|---|---|---|
| 1 | 215-630x6+190x11 | 210-765x6+155x10 | 0.6 | 0.6 | 0.8 | 0.4 | 0.2 | 100 | 3.15 | 3.32 | 56.4 | 4.2 | 27.4 | 90.5 |
| 2 | 260-555x8+185x12 | 245-625x9+150x11 | 0.7 | 0.9 | 1.3 | 0.6 | 0.2 | 99 | 2.97 | 3.12 | 59.3 | 5.9 | 27.4 | 97.1 |
| 3 | 235-645x6+165x14 | 225-560x8+165x12 | 0.1 | 0.3 | 0.3 | 0.0 | 0.5 | 99 | 2.82 | 2.84 | 59.1 | 1.3 | 27.4 | 95.0 |
| 4 | 225-690x6+190x10 | 220-725x6+170x9 | 0.4 | 0.4 | 0.5 | 0.3 | 0.0 | 99 | 3.27 | 3.44 | 56.3 | 2.8 | 27.4 | 88.1 |
| 5 | 205-635x6+180x12 | 215-645x6+175x10 | 0.6 | 0.8 | 1.2 | 0.5 | 0.3 | 99 | 3.02 | 3.19 | 57.1 | 5.5 | 27.4 | 93.8 |
| 6† | | | | | | | | | | | | | | |
| 7 | 220-685x6+200x9 | 225-760x6+180x8 | 0.0 | 0.0 | 0.0 | 0.0 | 0.0 | 100 | 3.45 | 3.51 | 55.8 | 0.0 | 27.4 | 84.1 |
| 8 | 190-650x6+195x10 | 235-775x6+175x8 | 0.4 | 0.4 | 0.6 | 0.3 | 0.0 | 100 | 3.21 | 3.38 | 55.9 | 3.1 | 27.4 | 88.4 |
| 9 | 165-575x6+195x12 | 230-635x6+175x10 | 0.5 | 0.5 | 1.3 | 0.4 | 0.0 | 100 | 3.11 | 3.28 | 57.3 | 4.9 | 27.4 | 92.4 |
| 10 | 130-720x6+195x11 | 285-730x6+170x10 | 0.5 | 0.6 | 0.8 | 0.4 | 0.2 | 100 | 3.04 | 3.21 | 57.7 | 4.3 | 27.4 | 93.0 |
| 11 | 130-750x6+180x12 | 330-550x8+165x12 | 0.5 | 0.8 | 0.9 | 0.3 | 0.2 | 100 | 2.85 | 2.94 | 60.1 | 4.5 | 27.4 | 98.5 |
| 12 | 150-755x6+165x14 | 300-560x8+155x13 | 0.1 | 0.2 | 1.0 | 0.1 | 0.4 | 100 | 2.82 | 2.83 | 60.2 | 2.9 | 27.4 | 97.7 |
| 13 | 180-735x6+180x12 | 340-685x6+175x10 | 0.3 | 0.4 | 0.6 | 0.3 | 0.0 | 100 | 3.28 | 3.38 | 58.5 | 3.1 | 27.4 | 90.6 |
| 14 | 145-820x6+185x11 | 235-710x6+165x11 | 0.5 | 0.7 | 1.0 | 0.5 | 0.2 | 100 | 2.92 | 3.06 | 57.8 | 5.0 | 27.4 | 95.4 |
| 15 | 205-760x6+190x11 | 340-490x7+185x12 | 0.0 | 0.0 | 0.3 | 0.0 | 0.0 | 100 | 2.82 | 2.82 | 60.4 | 0.7 | 27.4 | 95.7 |
| 16 | 160-805x6+200x9 | 250-800x6+185x8 | 0.0 | 0.0 | 0.0 | 0.0 | 0.0 | 100 | 3.41 | 3.57 | 56.5 | 0.0 | 27.4 | 84.8 |
| 17 | 115-745x6+200x10 | 270-735x6+170x10 | 0.5 | 0.5 | 0.6 | 0.3 | 0.0 | 100 | 3.16 | 3.33 | 57.3 | 3.4 | 27.4 | 90.5 |
| 18 | 120-740x6+185x12 | 315-640x6+175x11 | 0.4 | 0.6 | 0.9 | 0.3 | 0.1 | 99 | 2.95 | 3.11 | 58.8 | 4.2 | 27.4 | 95.1 |
| 19† | | | | | | | | | | | | | | |
| 20 | 175-705x6+185x10 | 210-715x6+185x8 | 0.0 | 0.0 | 0.0 | 0.0 | 0.0 | 100 | 2.82 | 2.87 | 55.8 | 0.0 | 27.4 | 90.4 |
| 21 | 195-650x6+215x9 | 215-710x6+185x8 | 0.0 | 0.0 | 0.0 | 0.0 | 0.0 | 100 | 3.43 | 3.60 | 55.9 | 0.0 | 27.4 | 84.2 |
| 22 | 170-535x9+170x22 | 200-595x12+135x20 | 1.4 | 1.7 | 2.3 | 1.3 | 0.6 | 98 | 3.59 | 3.73 | 66.1 | 10.1 | 27.4 | 104.1 |
| 23 | 250-540x8+200x15 | 215-595x10+170x13 | 1.1 | 1.5 | 1.9 | 1.2 | 0.4 | 99 | 3.61 | 3.76 | 62.7 | 9.7 | 27.4 | 100.2 |
| 24 | 155-745x6+210x13 | 235-765x8+175x11 | 0.6 | 0.7 | 1.0 | 0.5 | 0.4 | 89 | 3.70 | 3.82 | 60.5 | 5.4 | 27.4 | 93.6 |
| 25 | 225-555x6+195x12 | 240-630x6+190x9 | 0.0 | 0.1 | 0.0 | 0.0 | 0.0 | 100 | 2.82 | 2.82 | 57.4 | 0.1 | 27.4 | 92.1 |
| 26† | | | | | | | | | | | | | | |
| 27 | 170-665x6+205x9 | 215-700x6+185x8 | 0.0 | 0.0 | 0.0 | 0.0 | 0.0 | 100 | 2.85 | 2.95 | 55.7 | 0.0 | 27.4 | 89.6 |
| 28 | 250-605x6+185x12 | 230-600x6+200x8 | 0.0 | 0.0 | 0.0 | 0.2 | 0.1 | 100 | 2.82 | 2.82 | 115.1 | 0.8 | 54.7 | 177.8 |
| 29 | 210-550x6+190x13 | 245-595x6+185x10 | 0.0 | 0.0 | 0.1 | 0.0 | 0.2 | 99 | 2.82 | 2.85 | 116.1 | 0.6 | 54.7 | 178.6 |
| 30 | 190-635x6+210x9 | 225-740x6+180x8 | 0.3 | 0.3 | 0.4 | 0.2 | 0.0 | 100 | 3.08 | 3.25 | 111.5 | 4.5 | 54.7 | 173.8 |
| 31 | 190-525x10+175x20 | 195-600x12+145x19 | 1.6 | 1.9 | 2.5 | 1.5 | 0.5 | 99 | 2.89 | 3.06 | 66.2 | 11.5 | 0.0 | 83.5 |
| 32 | 230-585x10+250x15 | 230-525x8+200x16 | 1.0 | 1.6 | 1.7 | 1.1 | 0.0 | 90 | 2.95 | 3.11 | 67.7 | 9.8 | 0.0 | 82.2 |
| 33 | 230-580x7+230x13 | 245-490x7+180x13 | 0.7 | 0.8 | 1.3 | 0.6 | 0.4 | 97 | 2.85 | 3.02 | 61.3 | 6.1 | 0.0 | 74.0 |
| 34 | 215-630x6+180x12 | 225-685x6+190x8 | 0.0 | 0.1 | 0.1 | 0.1 | 0.1 | 100 | 3.09 | 3.09 | 56.5 | 0.6 | 51.3 | 111.4 |
| 35 | 225-635x6+190x11 | 215-700x6+165x10 | 0.0 | 0.0 | 0.0 | 0.0 | 0.0 | 99 | 3.09 | 3.10 | 56.8 | 0.0 | 51.3 | 111.1 |
| 36 | 205-655x6+195x10 | 230-765x6+175x8 | 0.0 | 0.0 | 0.0 | 0.0 | 0.0 | 100 | 3.12 | 3.22 | 55.9 | 0.0 | 51.3 | 109.9 |

The dimensions ($h_{c1}$, $b_c$, $t_{f,c}$, etc.) are given in mm unit; $C_0$, $C_1$, $C_2$ and $C_{LC}$ are given in 1000€ unit.
There was an additional constraint related to the minimum thickness of the web; the minimum considered plate thickness was 6mm in order to avoid problems related to corrosion and welding.
† There were numerical problems during the optimization procedure, the algorithm did not find stable solutions.

**Table 5** Optimized structural configurations ▲

**Fig. 9** Differences in the width-to-thickness ratio (slenderness) of the plate elements comparing to the optimized reference cases. ▼

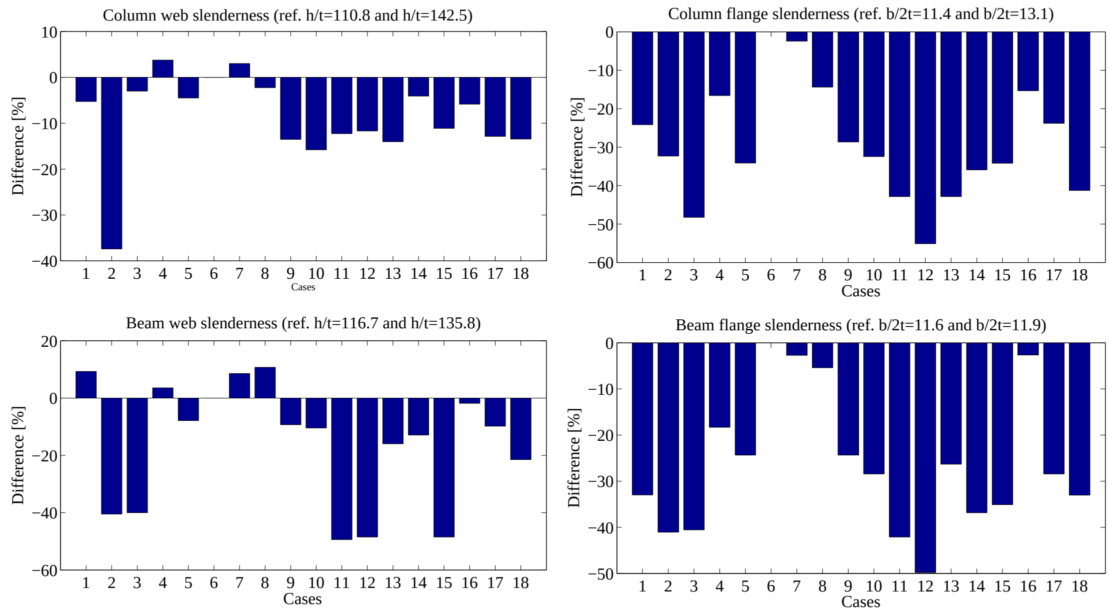

**JCSS [37]**

| Relative cost of safety measure | Consequences | | |
|---|---|---|---|
| | **Minor** | **Moderate** | **Large** |
| High | 1.67 | 1.98 | 2.55 |
| Moderate | 2.55 | 3.21 | 3.46 |
| Low | 3.21 | 3.46 | 3.83 |

**ISO 2394 [46]**

| Relative cost of safety measure | Consequences | | |
|---|---|---|---|
| | **Some** | **Moderate** | **Great** |
| High | 1.5 | 2.3 | 3.1 |
| Moderate | 2.3 | 3.1 | 3.8 |
| Low | 3.1 | 3.8 | 4.3 |

**EC0 [28]**

| Consequences | | |
|---|---|---|
| **Low (CC1)** | **Medium (CC2)** | **High (CC3)** |
| 3.3 | 3.8 | 4.3 |

**Table 6** Target reliability index values from standards and recommendations for 50 years service life

From the point-of-view of conceptual design stockier sections combined with less passive protection ensure better performance during fire. Less slender sections also give lower A/V value, thus the heating of these sections are slower comparing to sections which have higher A/V section ratio. Due to the fact that structural fire design is generally new for the structural designer society in Hungary, the issue of structural fire design is often assigned to fire safety engineers, who may be not well educated from the point-of-view of structural engineering, and select the amount of fire protection based only the section factor (A/V – ratio of perimeter and surface) supposing that the critical temperature of the element is e.g. 550 °C. It will be shown later in this section that this method is not reliable and not safe in some cases and the most economical solution cannot be achieved only with protection of slender elements that would be optimal in persistent design situation using thick passive protection. It is important to consider the fire design situation during structural design (and not after it) in order to achieve economical and well performing solutions.

The calculated optimum/target reliability indices are listed in Table 5. Comparing to the standardized target indices (in Table 6), it can be seen that the calculated values for cases #1 - #9 ($\beta$=2.82-3.45) are lower than the suggested values of EC0 [28]. It has to be noted that $\beta$=2.82 reliability index implies that the structure has almost 1.0 conditional failure probability in fire. In these cases the fire effect is too severe and the protection and strengthening of the structure may not be economical. $\beta$=2.82 reliability index is a lower bound because the occurrence of flashover is quite rare in the investigated case (Fig. 4). Due to the highly nonlinear, uncertain and extreme nature of the fire effect (especially when this nature is combined with extreme intensity, e.g. see fire curve #1 and #2 for R45 and R60 demand levels), ensuring of high reliability is too expensive (relative cost of safety measure is moderate or high), thus, the resulted reliability indices are low comparing to other cases. It has to be noted that some conservative assumptions have been made by the formulation of reliability analysis due to the lack of knowledge. By reducing this uncertainty and conservative assumptions, the calculated target reliability indices may be increased. The optimization procedures have been performed considering $\rho$=0.4 correlation coefficient (as a more likely value for the investigated structure) in Eq. (7), however, the reliability indices are presented for $\rho$=0.9 as well in Table 5, in order to characterize the effect of low and high correlation. With the consideration of higher correlation among the frames, higher reliability indices were calculated ($\beta$=2.84-3.51). These values better characterize smaller structures with smaller fire compartment. The difference between the probabilities of failure varied from 0% to -50%, thus the correlation has a significant effect on the reliability of the structure.

As it can be seen by comparing Table 5 and Table 6 and as it was pointed in [29], the target values of JCSS Probabilistic Model Code [37] and ISO 2394 standard [46] are more applicable for fire design of industrial steel tapered portal frames. Further issue is that the EC0 [28] does not give different groups according to the relative cost of safety measures, in this way, it recommends the same target reliability for persistent, seismic and fire design situation. This method may does not seem proper for providing solutions with consistent reliability which is one of the bases of safe and economic design.

It is a very important conclusion that the reliability indices related to optimum solutions are vary in a wide range when different fire curves and different time demands are considered during the design. This observation implies that the optimum safety level depends on the heating rate and the maximum temperature in the compartment. Furthermore, the safety level significantly depends on the occurrence of severe fire and flashover, thus it is dependent on the function of the building and the amount of active safety measures. This can be concluded on the basis of the optimization results of further cases as well (Table 5). For this reason, the safety of two identical frame structures is different when the function of the buildings is different. These conclusions predict the fact that comparable effects, such as ISO standard fire [16], cannot be the basis for consistent and reliable structural fire design. In order to achieve consistent reliability level, safe and economical solutions, it is important to model the fire effect as accurately as possible.

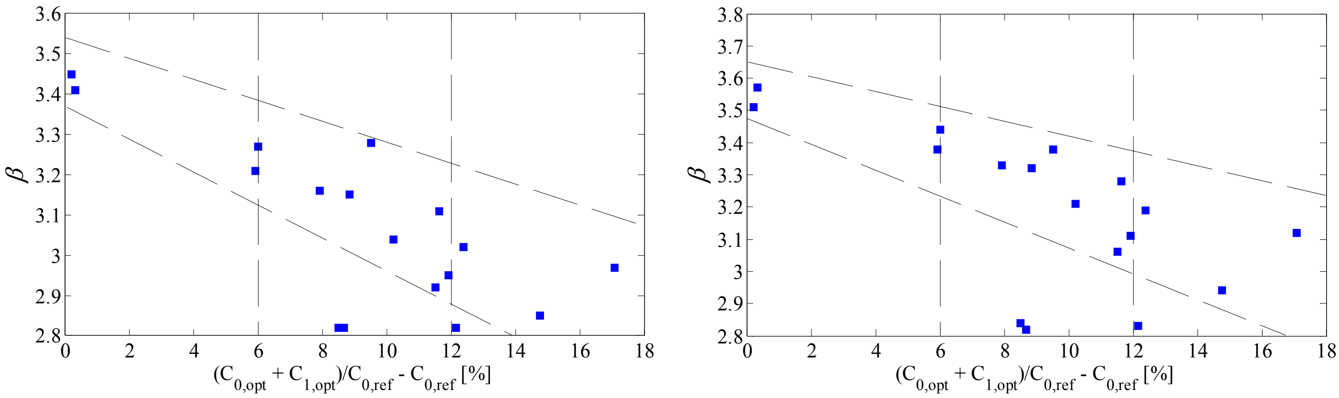


**Fig. 10** Optimal safety levels as a function of additional costs comparing to the configurations in Table 8: a) ρ=0.4; b) ρ=0.9 correlation coefficient

Based on the results of 36 optimized cases, a table with possible values for target reliability indices was constructed (Table 7), similarly to Table 6. The presented target indices may be valid for industrial steel portal frame structures with similar size and with similar function. Because of the consideration of low and high correlation (smaller structure/compartment) among the frames, the presented results cover a wide range of possible cases. Further investigation is necessary in order to define target indices for different type of structural configurations. Optimized cases with high initial cost components (Table 4, Fig. 10) or demanding fire curve are categorized in high relative cost of safety measure row, while cases optimized considering fire curve #3 resulted low additional costs (Fig. 10) are categorized in the last row. In Fig. 10 the initial costs of the optimized cases are compared with reference structures (Table 8), optimized in persistent design situation for 0.2 kN/m2 (column: 185-665x6+205x9, beam: 215-700x6+185x8) and 0.5 kN/m2 (column: 130-855x6+210x8, beam: 230-815x6+190x8) equipment load using the developed algorithm. Solutions with $\beta$=2.82 were not accounted because the fire effect and time demand were too severe in these cases. It can be seen that this table is in better agreement with the recommendations of JCSS and ISO 2394 than with EC0. Due to the limited number investigated cases, there is no defined range in columns related to minor and large consequences, thus further investigation is needed later in order to extend and validate the suggested numbers. It is still not clear what minor, moderate and large consequence implies and what is the method for selecting the appropriate consequence class. Based on engineering judgement, intermediate values may also be used. The consideration, that $C_{f,1}$= 30 m€ may be large, $C_{f,2}$ = 3 m€ may be moderate and $C_{f,3}$= 0.3 m€ may be minor consequence, is clearly related to the judgement of the authors. Considering solutions based on common design practice (cases #1-#9 in Table 8, $C_{s,init}=C_0+C_1+C_2\approx$90-100,000€), the considered failure costs were $C_f\approx$ 3 - 300$C_{s,init}$. Further investigation is necessary for better understanding the possible components (and their weights) of failure cost function. The target values are also influenced by the acceptance ability of the society and global economy of the country, so in some cases minimum limits may be used in order to ensure the minimum desired safety.

Compering the results of cases #2, #5 and #8 to results of cases #34, #35 and #36, it can be seen that the application of more active safety measures can result cheaper structure in terms of initial cost of steel superstructure and passive fire protection, however, active safety measures are generally expensive. It can be also concluded that life cycle cost values are lower with only alarm system, thus in the investigated case the application of both alarm and extinguish systems may not lead to economical design. Comparing to the results of cases #2, #5 and #8 to results of cases #31, #32 and #33, it can be concluded that the initial costs are much higher, nevertheless, they result the lowest life cycle costs (considering cases where the equipment load is 0.2 kN/m$^2$ and where the cost components are the same). In case of the investigated and similar structural configurations with storage function, optimal solution may be achieved with less active safety measure (if the presented safety level meets the allowable minimum safety limit), but with more passive fire protection and stronger structure. This conclusion is in good agreement with the results of an earlier study [29].

**50 years service life: calculated target reliability indices**

| Relative cost of safety measure | Fire effect severity | Minor consequences | Moderate consequences | Large consequences |
|---|---|---|---|---|
| High | High | 2.8 (**2.8**)* | 2.8 – 3.2 (**2.8 – 3.3**) | 3.6 (**3.7**)* |
| Moderate | Medium | 2.8 (**2.9**)*† | 2.9 – 3.4 (**3.0 – 3.5**) | 3.6 (**3.8**)* |
| Low | Low | 2.9 (**3.0**)* | 3.1 – 3.5 (**3.3 – 3.6**) | 3.7 (**3.8**)* |

* based on limited number of cases, further investigation is necessary; † interpolated

**Table 7** Calculated target reliability indices for tapered portal frames with storage function (with ρ=0.4 and ρ=0.9 correlation coefficient)

In order to investigate the achievable performance using common practice in structural fire engineering, the passive protection of the above mentioned reference frames, which have been optimized considering only constraints related to persistent design situation, is selected based only on the section factor of the sections and according to the producer's manual [23], assuming that the critical temperature is 550C°.

The A/V factor in case of the columns is between 250 and 303 1/m, while in case of the beams it vary from 280 to 305 1/m. The calculated reliability indices and life cycle costs can be seen in Table 8.

The calculated reliability indices vary in a wide range and they rarely achieve the EC0 recommended $\beta$ target indices because of several reasons: a) the structural fire design is characterized by high degree of uncertainty, the EC0 recommended target indices may not refer well to extreme situations; b) the design of intumescent coating is based and generally the fire design is often based on ISO standard fire curve which is not able to represent real fire thus cannot be used as the basis for consistent, safe and economical structural fire design; the reliability depends on the quantity and quality of the combustible materials and depends on the function of the building; c) the reliability of a structural system is generally lower than the reliability of separated elements (structural reliability is often calculated for separated elements in the literature, e.g. in [47], [48] and [49]); d) the structural fire design should be completed by the structural designer and should be included in the design process from the beginning of searching possible economic solutions; e) the persistent design situation and fire design situation may be contradictory objectives in some cases, the cross section (see Table 5 and 8; compare e.g. cases #1 - #3 or cases #10 - #12) which is close to optimum for conventional loads is not optimum for fire design; f) the common practice that the passive protection is selected after the persistent design assuming the critical temperature of the element may be unreliable (Fig. 11) and unsafe.

**Table 8** Persistent design situation optimized structural configurations in fire design situation

| # | $h_{c1}$ - $h_{c2}$ x $t_{w,c}$ + $b_c$ x $t_{f,c}$ | $h_{b1}$ - $h_{b2}$ x $t_{w,b}$ + $b_b$ x $t_{f,b}$ | $t_{p,c1}$ | $t_{p,c2}$ | $t_{p,b2}$ | $t_{p,b1}$ | $t_{p,c}$ | $\beta$ 0.4 | $\beta$ 0.9 | $C_0$ | $C_1$ | $C_2$ | $C_{LC}$ | $\Delta C_{LC}$ [%]† |
|---|---|---|---|---|---|---|---|---|---|---|---|---|---|---|
| 1 | 185-665x6+205x9 | 215-700x6+185x8 | 0.54 | 0.58 | 0.61 | 0.58 | 0.6 | 2.97 | 3.12 | 55.7 | 4.2 | 27.4 | 91.8 | 1.4 |
| 2 | 185-665x6+205x9 | 215-700x6+185x8 | 1.38 | 1.48 | 1.57 | 1.48 | 1.5 | 2.89 | 3.02 | 55.7 | 10.8 | 27.4 | 99.7 | 2.7 |
| 3 | 185-665x6+205x9 | 215-700x6+185x8 | 2.15 | 2.30 | 2.47 | 2.30 | 2.4 | 2.84 | 2.92 | 55.7 | 16.9 | 27.4 | 106.8 | 12.3 |
| 4 | 185-665x6+205x9 | 215-700x6+185x8 | 0.54 | 0.58 | 0.61 | 0.58 | 0.6 | 3.13 | 3.24 | 55.7 | 4.2 | 27.4 | 89.9 | 2.1 |
| 5 | 185-665x6+205x9 | 215-700x6+185x8 | 1.38 | 1.48 | 1.57 | 1.48 | 1.5 | 3.01 | 3.18 | 55.7 | 10.8 | 27.4 | 97.8 | 4.3 |
| 6 | 185-665x6+205x9 | 215-700x6+185x8 | 2.15 | 2.30 | 2.47 | 2.30 | 2.4 | 2.89 | 3.02 | 55.7 | 16.9 | 27.4 | 78.4 | |
| 7 | 185-665x6+205x9 | 215-700x6+185x8 | 0.54 | 0.58 | 0.61 | 0.58 | 0.6 | 3.52 | 3.67 | 55.7 | 4.2 | 27.4 | 88.0 | 4.6 |
| 8 | 185-665x6+205x9 | 215-700x6+185x8 | 1.38 | 1.48 | 1.57 | 1.48 | 1.5 | 3.40 | 3.56 | 55.7 | 10.8 | 27.4 | 94.9 | 7.4 |
| 9 | 185-665x6+205x9 | 215-700x6+185x8 | 2.15 | 2.30 | 2.47 | 2.30 | 2.4 | 3.16 | 3.33 | 55.7 | 16.9 | 27.4 | 102.4 | 10.8 |
| 10 | 130-855x6+210x8 | 230-815x6+190x8 | 0.68 | 0.72 | 0.72 | 0.67 | 0.7 | 2.95 | 3.10 | 56.3 | 5.5 | 27.4 | 93.9 | 1.0 |
| 11 | 130-855x6+210x8 | 230-815x6+190x8 | 1.80 | 1.90 | 1.90 | 1.77 | 1.9 | 2.86 | 2.97 | 56.3 | 14.5 | 27.4 | 104.5 | 6.1 |
| 12 | 130-855x6+210x8 | 230-815x6+190x8 | 2.35 | 2.50 | 2.50 | 2.30 | 2.5 | 2.83 | 2.88 | 56.3 | 18.9 | 27.4 | 109.5 | 12.1 |
| 13 | 130-855x6+210x8 | 230-815x6+190x8 | 0.68 | 0.72 | 0.72 | 0.67 | 0.7 | 3.24 | 3.41 | 56.3 | 5.5 | 27.4 | 91.0 | 0.4 |
| 14 | 130-855x6+210x8 | 230-815x6+190x8 | 1.80 | 1.90 | 1.90 | 1.77 | 1.9 | 2.96 | 3.11 | 56.3 | 14.5 | 27.4 | 102.8 | 7.7 |
| 15 | 130-855x6+210x8 | 230-815x6+190x8 | 2.35 | 2.50 | 2.50 | 2.30 | 2.5 | 2.85 | 2.95 | 56.3 | 18.9 | 27.4 | 109.1 | 14.0 |
| 16 | 130-855x6+210x8 | 230-815x6+190x8 | 0.68 | 0.72 | 0.72 | 0.67 | 0.7 | 3.46 | 3.62 | 56.3 | 5.5 | 27.4 | 90.0 | 6.1 |
| 17 | 130-855x6+210x8 | 230-815x6+190x8 | 1.80 | 1.90 | 1.90 | 1.77 | 1.9 | 3.35 | 3.51 | 56.3 | 14.5 | 27.4 | 99.4 | 9.8 |
| 18 | 130-855x6+210x8 | 230-815x6+190x8 | 2.35 | 2.50 | 2.50 | 2.30 | 2.5 | 3.08 | 3.25 | 56.3 | 18.9 | 27.4 | 105.7 | 11.1 |
| 19 | 185-665x6+205x9 | 215-700x6+185x8 | - | - | - | - | - | 2.82 | 2.83 | 55.7 | 0.0 | 27.4 | 90.3 | |
| 20 | 185-665x6+205x9 | 215-700x6+185x8 | - | - | - | - | - | 2.82 | 2.87 | 55.7 | 0.0 | 27.4 | 90.3 | -0.1 |
| 21 | 185-665x6+205x9 | 215-700x6+185x8 | - | - | - | - | - | 3.34 | 3.50 | 55.7 | 0.0 | 27.4 | 84.4 | 0.2 |
| 22 | 185-665x6+205x9 | 215-700x6+185x8 | 1.38 | 1.48 | 1.57 | 1.48 | 1.5 | 2.89 | 3.02 | 55.7 | 10.8 | 27.4 | 151.7 | 39.7 |
| 23 | 185-665x6+205x9 | 215-700x6+185x8 | 1.38 | 1.48 | 1.57 | 1.48 | 1.5 | 3.01 | 3.18 | 55.7 | 10.8 | 27.4 | 133.1 | 27.5 |
| 24 | 185-665x6+205x9 | 215-700x6+185x8 | 1.38 | 1.48 | 1.57 | 1.48 | 1.5 | 3.40 | 3.56 | 55.7 | 10.8 | 27.4 | 104.0 | 7.8 |
| 25 | 185-665x6+205x9 | 215-700x6+185x8 | 1.38 | 1.48 | 1.57 | 1.48 | 1.5 | 2.89 | 3.02 | 55.7 | 10.8 | 27.4 | 94.5 | 10.4 |
| 26 | 185-665x6+205x9 | 215-700x6+185x8 | 1.38 | 1.48 | 1.57 | 1.48 | 1.5 | 3.01 | 3.18 | 55.7 | 10.8 | 27.4 | 94.3 | |
| 27 | 185-665x6+205x9 | 215-700x6+185x8 | 1.38 | 1.48 | 1.57 | 1.48 | 1.5 | 3.40 | 3.56 | 55.7 | 10.8 | 27.4 | 94.0 | 12.3 |
| 28 | 185-665x6+205x9 | 215-700x6+185x8 | 1.38 | 1.48 | 1.57 | 1.48 | 1.5 | 2.89 | 3.02 | 111.4 | 22.5 | 54.7 | 194.4 | 9.3 |
| 29 | 185-665x6+205x9 | 215-700x6+185x8 | 1.38 | 1.48 | 1.57 | 1.48 | 1.5 | 3.01 | 3.18 | 111.4 | 22.5 | 54.7 | 192.5 | 7.8 |
| 30 | 185-665x6+205x9 | 215-700x6+185x8 | 1.38 | 1.48 | 1.57 | 1.48 | 1.5 | 3.40 | 3.56 | 111.4 | 22.5 | 54.7 | 189.6 | 9.1 |
| 31 | 185-665x6+205x9 | 215-700x6+185x8 | 1.38 | 1.48 | 1.57 | 1.48 | 1.5 | 1.93 | 2.11 | 55.7 | 10.8 | 0.0 | 146.9 | 76.0 |
| 32 | 185-665x6+205x9 | 215-700x6+185x8 | 1.38 | 1.48 | 1.57 | 1.48 | 1.5 | 2.10 | 2.32 | 55.7 | 10.8 | 0.0 | 120.1 | 46.0 |
| 33 | 185-665x6+205x9 | 215-700x6+185x8 | 1.38 | 1.48 | 1.57 | 1.48 | 1.5 | 2.61 | 2.80 | 55.7 | 10.8 | 0.0 | 80.1 | 8.2 |
| 34 | 185-665x6+205x9 | 215-700x6+185x8 | 1.38 | 1.48 | 1.57 | 1.48 | 1.5 | 3.15 | 3.27 | 55.7 | 10.8 | 51.3 | 120.3 | 7.9 |
| 35 | 185-665x6+205x9 | 215-700x6+185x8 | 1.38 | 1.48 | 1.57 | 1.48 | 1.5 | 3.27 | 3.42 | 55.7 | 10.8 | 51.3 | 119.4 | 7.5 |
| 36 | 185-665x6+205x9 | 215-700x6+185x8 | 1.38 | 1.48 | 1.57 | 1.48 | 1.5 | 3.64 | 3.79 | 55.7 | 10.8 | 51.3 | 118.2 | 7.5 |

The dimensions ($h_{c1}$, $b_c$, $t_{f,c}$, etc.) are given in mm unit; $C_0$, $C_1$, $C_2$ and $C_{LC}$ are given in 1000€ unit. The last column shows the difference in $C_{LC}$. The structures have been optimized considering only dead, equipment and meteorological loads, thus the D/C ratio of every configuration is 100% in persistent design situation.

† Compared to Table 5; positive value means that cases optimized in persistent design situation resulted higher life cycle cost.

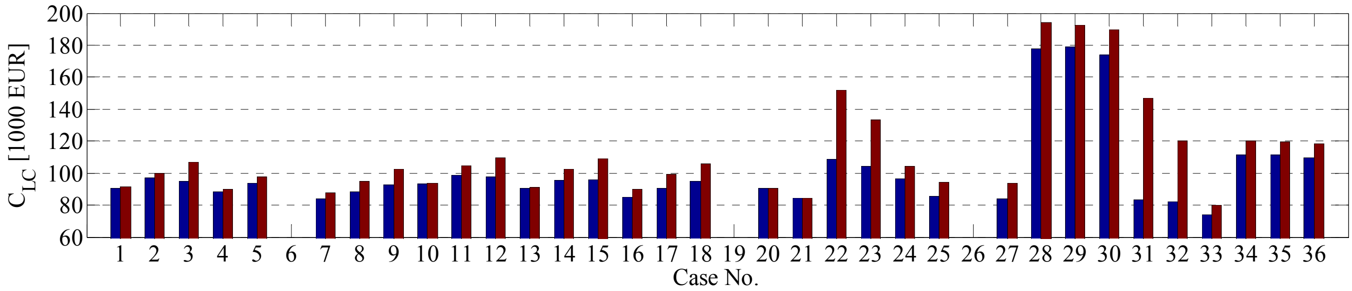


**Fig. 11** The life cycle costs of optimized (blue) and reference cases (red)

The life cycle cost values are higher than the values in Table 5 for optimized cases (Fig. 11); the achievable saving for life cycle with the presented method varies from -0.1 to +43.2% comparing to the common design practice. There is no correlation between the difference in probability of failure and the difference in life cycle cost, thus the common practice is unreliable in case of severe and less severe effects, as well. The difference in probability of failure varies between -85 and +1290%, the highest negative values have been calculated for fire curve #3. In most of the cases the difference is positive and significant positive differences can be observed for R45 and R60 time demands, especially when the fire effect is severe or extreme (fire curves #1 and #2 , respectively). It shows that the common practice and the application of ISO standard curve are unsafe in lot of cases.

Related to the protection of connections, it was observed that the protection thicknesses at the beam-to-column connections are much lower in case of the optimized cases than in cases presented in Table 8, where the thicknesses are selected based on the thicknesses of connected elements which would be a reasonable engineering decision if it was a real design situation. Due to the generally slender structural configuration and due to the fact that the Young's modulus decreases at high temperature, the leading failure mode in fire design situation is loss of stability of main elements. Furthermore the heating of connection zones is slower than the heating of connected elements. Thus, the beam-to-column connections are not fully utilized in fire design situation and there is no need for thick protection in the connection zones. However, the heating of the connections is generally more uncertain and thicker protection does not mean significant additive cost, for this reason, an engineering practice according to which the connection is protected as the connected elements can be considered safe and good in the case of the investigated structure and structural configuration.

## 7 Conclusions and optimal design of tapered portal frames

In this paper, the optimal fire design of steel tapered portal frames is presented. Covering large number of possible design cases, within the framework of a parametric study optimal solutions are analysed in terms of structural safety, cost effectiveness and structural configuration. The developed methodology and algorithm are comprehensive and complex; its details are discussed in details in [22]. The connection of structural optimization with complex structural reliability analysis for fire design is new and cannot be found in the literature. The ability of developed algorithm combined with the presented method to find optimal solutions is investigated within a sensitivity analysis, in which the parameters of applied genetic algorithm are set.

From the variation of the presented optimized solutions, it can be observed that the developed algorithm seeks the solutions in large search space. During an optimization process, the algorithm analyses large number of possible design alternatives. The finding of global optimum cannot be proven mathematically because of the high degree of nonlinearity, the discrete nature of the design problem and the heuristic nature of GA, nevertheless, this fact has no significant importance from practical point-of-view and the resulted solutions can be considered optimal solutions which have been found after analysing thousands of possible design alternatives.

The aim of this study was to derive useful recommendations and design concepts related to optimal structural safety, design practice and structural configuration based on the results of a parametric study. Instead of finding configurations with slightly lower initial cost, deriving well performing, reliable and also cost effective solutions has more importance from practical point-of-view. The presented results and suggestions may be valid for only industrial steel portal frame structures with similar size and with similar function to the investigated frame. Further investigation is necessary in order to define rules and target indices for different type of structural configurations.

### 7.1 Optimal, target safety of tapered frames in fire design situation

- Possible target reliability indices have been derived for structural fire design of steel tapered portal frame structures. The presented values (Table 7) are generally lower than the target indices in EC0 standard and they are better agreement with the suggestions of JCSS and ISO 2394. Further research is important later in order to extend and validate the suggested numbers (especially for other functions and structural configurations) and in order to understand better the components of failure costs ($C_f$). The target reliability indices may be also influenced by the acceptance ability of the society and global economy of the country, so in some cases minimum limits may be used in order to ensure the minimum desired safety.

- Further issue is that the EC0 does not differentiate groups according to the relative cost of safety measures, in this way, it recommends the same target reliability for persistent, seismic and fire design situation. For example, the structural fire design is characterized by high degree of uncertainty, the EC0 recommended target indices may not refer well to extreme situations. This method does not seem to be able to provide solutions with consistent reliability which is one of the bases of safe and economic design.
- With the consideration of higher correlation among the frames, higher reliability indices were calculated. These values better characterize smaller structures or structures with smaller fire compartment. The difference between the probabilities of failure varied from 0% to -50%, thus this issue has a significant effect on the reliability of the structure. Furthermore, with reducing the size of the compartment, the possibility of fire occurrence can be decreased.

## 7.2 Structural fire design practice of tapered frame structures

- The optimal design considering conventional and fire effects may be contradictory objectives thus the consideration of fire design situation during the seeking optimal solutions in the design process will change the resulted configurations and dimensions. Economical solutions cannot be achieved only with protection slender elements, which are adequate in persistent design situation, using thick passive protection layers. This common practice is unreliable and unsafe as the presented results have proven. The structural fire design should be done by structural designers and it is important to consider the fire design situation during structural design from the conceptual design in order to achieve economical and well performing solutions.
- Through the severity of the fire, the structural reliability depends on the quality and quantity of combustible materials, the compartment geometry, the active safety measures and the function of the building. For this reason, the application of comparable effects, such as ISO standard fire [16], cannot be the basis for consistent and reliable structural fire design. In order to achieve consistent reliability level, safe and economical solutions, it is important to model the fire effect as accurately as possible.

## 7.3 Conceptual design of tapered frame structures

- As it was also pointed in [29], it is not safe and economical to ensure the fire safety of the investigated frames without passive fire protection because the steel plates are very heat conductive and their stiffness and strength are decreased very quickly in severe fire.
- Due to relatively high initial and maintenance costs, in case of the investigated and similar structural configurations with storage function, life cycle optimal solution may be achieved with less active safety measure, but with more passive fire protection and stronger structure. Another issue related to the application of active safety measures that their effect on the structural reliability should be incorporated in the design process. For this purpose, there is a method in EC1-1-2 [14] standard in case of which the design fire load can be modified with factors based upon e.g. the amount of active safety measures.
- The less slender, stockier sections (with lower plate width-to-thickness ratio) are more appropriate in severe fire effect (especially with high time demand) due to the fact that the structure is sensitive for stability failure. These sections, combined with less passive fire protection ensure better performance and safety in fire. Less slender sections also give lower A/V value, thus the heating of these sections are slower comparing to sections which have higher A/V section ratio.
- As regards to the connections, it was observed that the beam-to-column connections are not fully utilized in fire design situation and there is no need for thick protection in the connection zones. However, the heating of the connections is generally more uncertain and thicker protection does not mean significant additive cost, for this reason, an engineering practice according to which the connection is protected as the connected elements can be considered safe and appropriate in the case of the investigated structure and structural configuration.
- In order to reduce the occurrence of fire and to increase the structural reliability, it is favourable to reduce the fire compartment size.

## Acknowledgement

This paper was supported by the János Bolyai Research Scholarship of the Hungarian Academy of Sciences. The presented results are part of the “HighPerFrame” R&D project Nr. GOP-1.1.1-11-2012-0568, supported by the Új Széchenyi Terv.

## References

[1] K. Thomas, H. Tam, A. Jennings, Optimal plastic design of frames with tapered members, Computers & Structures, 30(1988) 537-544. DOI: http://dx.doi.org/10.1016/0045-7949(88)90287-8

[2] M. S. Hayalioglu, M. P. Saka, Optimum design of Geometrically nonlinear elastic-plastic steel frames with tapered members, Computers & Structures, 44(1992) 915-924. DOI: http://dx.doi.org/10.1016/0045-7949(92)90479-J
[3] M. P. Saka, Optimum design of steel frames with tapered members, Computers & Structures, 63(1997) 797-811. DOI: http://dx.doi.org/10.1016/S0045-7949(96)00074-0
[4] S. Kravanja, G. Turkalj, S. Silih, T. Zula, Optimal design of single-story steel building structures based on parametric MINLP optimization, Journal of Constructional Steel Research, 81(2013) 86-103. DOI: http://dx.doi.org/10.1016/j.jcsr.2012.11.008
[5] S. Kravanja, T. Zula, Cost optimization of industrial steel building structures, Advances in Engineering Software, 41(2001) 442-450. DOI: http://dx.doi.org/10.1016/j.advengsoft.2009.03.005
[6] D. T. Phan, J. B.P. Lim, T. T. Tanyimboh, R. M. Lawson, Y. Xu, S. Martin, W. Sha, Effect of serviceability limits on optimal design of steel portal frame, Journal of Constructional Steel Research, 86(2013) 74-84. DOI: http://dx.doi.org/10.1016/j.jcsr.2013.03.001
[7] R. McKinstray, J. B.O. Lim, T. T. Tanyimboh, D. T. Phan, W. Sha, Optimal design of long-span steel portal frames using fabricated beams, Journal of Constructional Steel Research, 104(2015) 104-114. DOI: http://dx.doi.org/10.1016/j.jcsr.2014.10.010
[8] P. Hadril, M. Mielonen, L. Fülöp, Advanced design and optimization of steel portal frames, Journal of Structural Mechanics, 43(2010) 44-60.
[9] T. Balogh, L. G. Vigh, Seismic reliability based optimization of steel portal frame structures, Proceedings of SECED 2015 Conference: Earthquake Risk and Engineering towards a Resiliant World, Cambridge, United Kingdom, 2015.
[10] Liu Z, Atamturktur S, Juang CH (2014). Reliability based multi-objective robust design optimization of steel moment resisting frame considering spatial variability of connection parameters. Engineering Structures, 76, pp. 393-403. DOI: http://dx.doi.org/10.1016/j.engstruct.2014.07.024
[11] Lin KC, Lin CCJ, Chen JY, Chang HY (2010) Seismic reliability of steel framed buildings. Structural Safety, 32, pp. 174-182. DOI: http://dx.doi.org/10.1016/j.strusafe.2009.11.001
[12] H. A. Rojas, C. Foley, S. Pezeshk, Risk-Based Design for Optimal Structural and Nonstructural System Performance, Earthquake Spectra, 27(2011) 857-880. DOI: http://dx.doi.org/10.1193/1.3609877
[13] K. Jármai, Optimization of a Steel Frame for Fire Resistance with and without Protection, Proceedings of Design, Fabrication and Economy of Welded Structures International Conference, pp. 79-89., Miskolc, Hungary, 2008. DOI: http://dx.doi.org/10.1533/9781782420484.2.79
[14] MSZ EN 1991-1-2:2005, Eurocode 1: Actions on structures – Part 1-2: General actions – Actions on structures exposed to fires, Hungarian Standards Institution. Budapest, Hungary.
[15] MSZ EN 1993-1-2:2013, Eurocode 3: Design of steel structures – Part 1-2: General rules – Structural fire design, Hungarian Standards Institution. Budapest, Hungary.
[16] ISO 834 – 10: 2014. Fire resistance tests – Elements of building constructions.
[17] T. Balogh, L. G. Vigh, Optimal design of tapered steel portal frame structures subjected to fire effects (in Hungarian), MAGÉSZ Steel Structures, 1. Special Issue (2015) 84-94.
[18] R. V. Coile, R. Caspelle, L. Taerwe, Lifetime Cost Optimization for the Structural Fire Resistance of Concrete Slabs, Fire Technology, 50(2014) 1201-1227. DOI: http://dx.doi.org/10.1007/s10694-013-0350-9
[19] L. Dunai, Z. Papp, High Performance Steel Structural System – HighPerFrame Research and Development Project (in Hungarian), MAGÉSZ Steel Structures, 1. Special Issue (2015) 3-5.
[20] L. Horváth, B. Kövesdi, Innovative design methods and solutions in fire design of steel frames (in Hungarian) , MAGÉSZ Steel Structures, 1. Special Issue (2015) 13-20.
[21] MSZ EN 1993-1-8:2012, Eurocode 3: Design of steel structures – Part 1-8: Design of joints, Hungarian Standards Institution. Budapest, Hungary.
[22] T. Balogh, L. G. Vigh, Complex and comprehensive method for reliability calculation of structures under fire exposure, Fire Safety Journal, Under review
[23] Dunamenti Ltd., Technical data sheet of Polylack A intumescent painting (in Hungarian), http://www.dunamenti.hu/, 2015.
[24] MSZ EN 13381-8:2015. Test methods for determining the contribution to the fire resistance of structural members – Part 8: Applied reactive protection to steel members, Hungarian Standards Institution. Budapest, Hungary.
[25] G. Q. Li, G. B. Lou, C. Zhang, L. L. Wang, Y. C. Wang. Assess the Fire Resistance of Intumescent Coatings by Equivalent Constant Thermal Resistance. Fire Technology, 48, pp. 529-546, 2012. DOI: http://dx.doi.org/10.1007/s10694-011-0243-8
[26] European Commission for Constructional Steelwork (ECCS), Design manual on the European recommendation for the fire safety of steel structures. Brussels (1985).
[27] T. Balogh, L. G. Vigh, Reliability calculation of portal frame structures exposed extreme loading conditions with First Order Reliability Method (in Hungarian), Proceedings of 12th Hungarian Conference on Mechanics (XII. MAMEK), Miskolc, Hungary, 2015.
[28] MSZ EN 1990:2011, Eurocode 0, Basis of structural design, Hungarian Standards Institution, Budapest, Hungary.
[29] T. Balogh, L. G. Vigh, Optimum reliability of a steel tapered portal frame structure exposed to fire, Proceedings of 4th Application of Structural Fire Engineering Conference, Dubrovnik, Croatia, 2015.
[30] M. Holickỳ, The target reliability and working life, in Safety and Security Engineering IV, Southempton, Boston, USA: WIT Press, 2011.
[31] J. F. Cadorin, D. Pintea, J. M. Franssen, The Design Fire Tool OZone V2.0 – Theoretical Description and Validation On Experimental Fire Tests, 1st draft, University of Liege, Belgium, 2001.
[32] DIFISEK Program: Dissemination of Fire Safety Engineering Knowledge documents - WP1 Thermal and mechanical actions.
[33] M. H. Faber, Risk and Safety in Engineering – Lecture notes, ETH Zürich, 2009.
[34] S. K. Choi, R. V. Grandhim, R. A. Canfield, Reliability-based Srtuctural Design, Springer-Verlag, London, 2007.
[35] Opensees Developers Group of University of Edinburgh, OpenSeesThermal, www.wiki.ed.ac.uk/display/opensees/UoE+OpenSees
[36] MSZ EN 1993-1-1:2009, Eurocode 3, Design of steel structures – Part 1-1: General rules and rules for buildings, Hungarian Standards Institution, Budapest, Hungary.
[37] Joint Committee on Structural Safety (JCSS), Probabilistic Model Code, 2000.
[38] MSZ EN 1991-1-3:2005, Eurocode 1: Actions on structures – Part 1-3: General actions – Snow loads, Hungarian Standards Institution. Budapest, Hungary.
[39] MSZ EN 1991-1-4:2007, Eurocode 1: Actions on structures – Part 1-4: General actions – Wind loads, Hungarian Standards Institution. Budapest, Hungary.
[40] Leonardo da Vinci Pilot Project, Implementation of Eurocodes – Reliability backgorunds (Handbook 2), Prague, 2005.
[41] S. Szalai, T. Antofie, P. Barbosa, Z. Bihari, M. Lakatos, J. Spinoni, T. Szentimrey, and J. Vogt, The CARPATCLIM project: creation a gridded Climate Atlas of the Carpathian Region for 1961-2010 and its use in the European Drought Observatory of JRC. 12th EMS Annual Meeting and 9th European Conference on Applied Climatology (ECAC), Lodz, Poland, 10 – 14 September 2012.

[42] M. Sỳkora, Reliability Analysis of a Steel Frame, Acta Polytechnica 42(2002) 27-34.
[43] Goldberg D. E., Genetic Algorithm in Search, Optimization, and Machine Learning, Kluwer Academic Publishers, Boston, MA, USA, 1989.
[44] T. Balogh, M. D'Aniello, L. G. Vigh, R. Landolfo, Performance Based Design Optimization of Steel Concentric Braced Structures. Eurosteel 2014: 7th European Conference on Steel and Composite Structures, Naples, Italy. 2014.09.10. - 2014.09.12.
[45] C. Y. Lin and W. H. Wu, Self-organizing adaptive penalty strategy in constrained genetic search. Structural and Multidisciplinary Optimization. 26(2004). p. 417-428. DOI: http://dx.doi.org/10.1007/s00158-003-0373-9
[46] ISO 2394:2015, General principles on reliability for structures
[47] C. Zhang, G. Q. Li, Y. C. Wang. Probabilistic analysis of steel columns protected by intemescent coating subjected to natural fires, Structural Safety, 50, pp. 16-26, 2014. DOI: http://dx.doi.org/10.1016/j.strusafe.2014.03.005
[48] Leonardo Da Vinci Pilot Project CZ/02/B/F/PP-134007. Implementation of Eurocodes, Handbook 5: Design of buildings for the fire situation.
[49] H. Gulvanessian, M. Holicky, L. G. Cajot, J. B. Schleich. Reliability Analysis of a steel beam under fire design situation, Proceedings of the 2nd European Conference on Steel and Composite Structures, Eurosteel 1999, pp. 177-180, Prague, Czech Republic.
[50] V. Nadolski and M. Sykora, Model uncertainties of steel members. In Proc. the ESREL 2015 European Safety and Reliability Conference, 7-10 September, 2014, Zürich, Switzerland.